UNSW Seminar, 8.11.2024

Susan Schorr

Structural disorder in photovoltaic absorber materials

Helmholtz-Zentrum Berlin für Materialien und Energie, Department Structure and Dynamics of Energy Materials, Germany
Freie Universität Berlin, Institute of Geological Sciences, Germany

Helmholtz Association in Germany

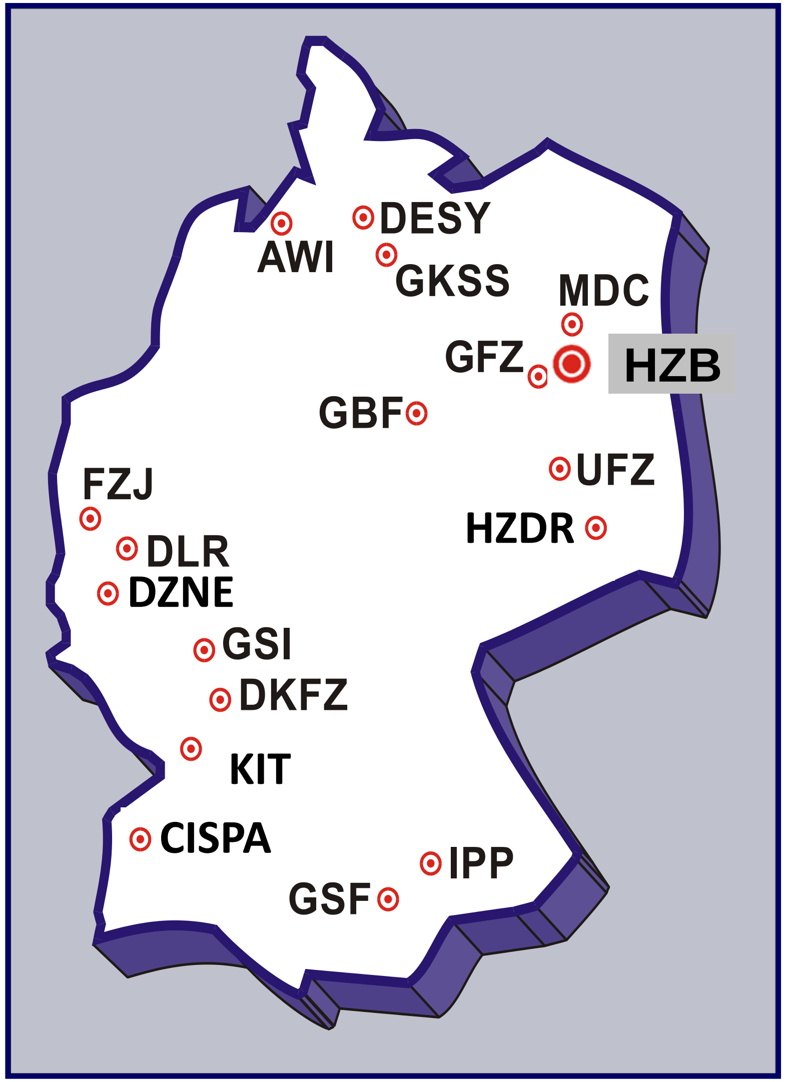

The Helmholtz Association is one of the large research associations in Germany, contributing to solving grand challenges facing society, science and industry
by conducting top-rate research in the fields of
Aeronautics, Space and Transport; Earth and Environment; Energy; Health; Matter; and Information.

- 18 legally independent Research Centers across Germany
- centers design and maintain numerous powerful large-scale facilities
- 46.000 employees
- annual budget of 6 billion Euros

Helmholtz-Zentrum Berlin fuer Materialien und Energie … HZB
large scale faciliy → synchrotron radiation faciliy BESSYII

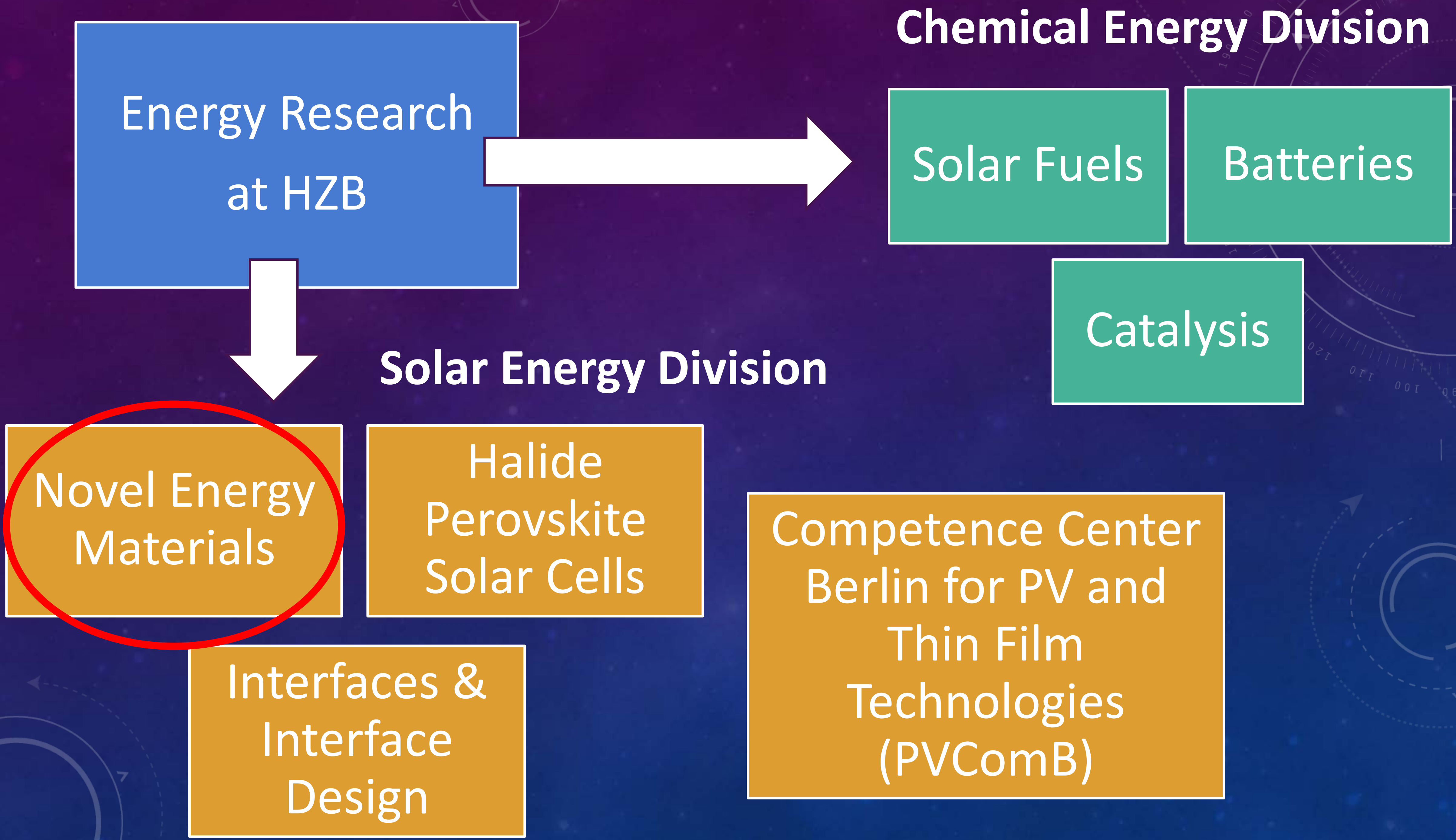

Energy Research at HZB

Chemical Energy Division

Solar Fuels

Batteries

Catalysis

Solar Energy Division

Novel Energy Materials

Halide Perovskite Solar Cells

Interfaces & Interface Design

Competence Center Berlin for PV and Thin Film Technologies (PVComB)

Synthesis of Photovoltaic Absorber Materials

Christiane Stephan-Scherb in the powder synthesis lab

- **Synthesis/growth of multinary compound semiconductors (chalcogenides, nitrides, metal halides)**
- **New energy materials are also synthesized as reference materials and made available to our cooperation partners**
- **Advanced structural and optical characterisation**
- **Advanced structural characterisation using large scale facilites (synchrotron X-rays, neutrons)**

Novel semiconductors with non-toxic, abundant constituents and long-time stability

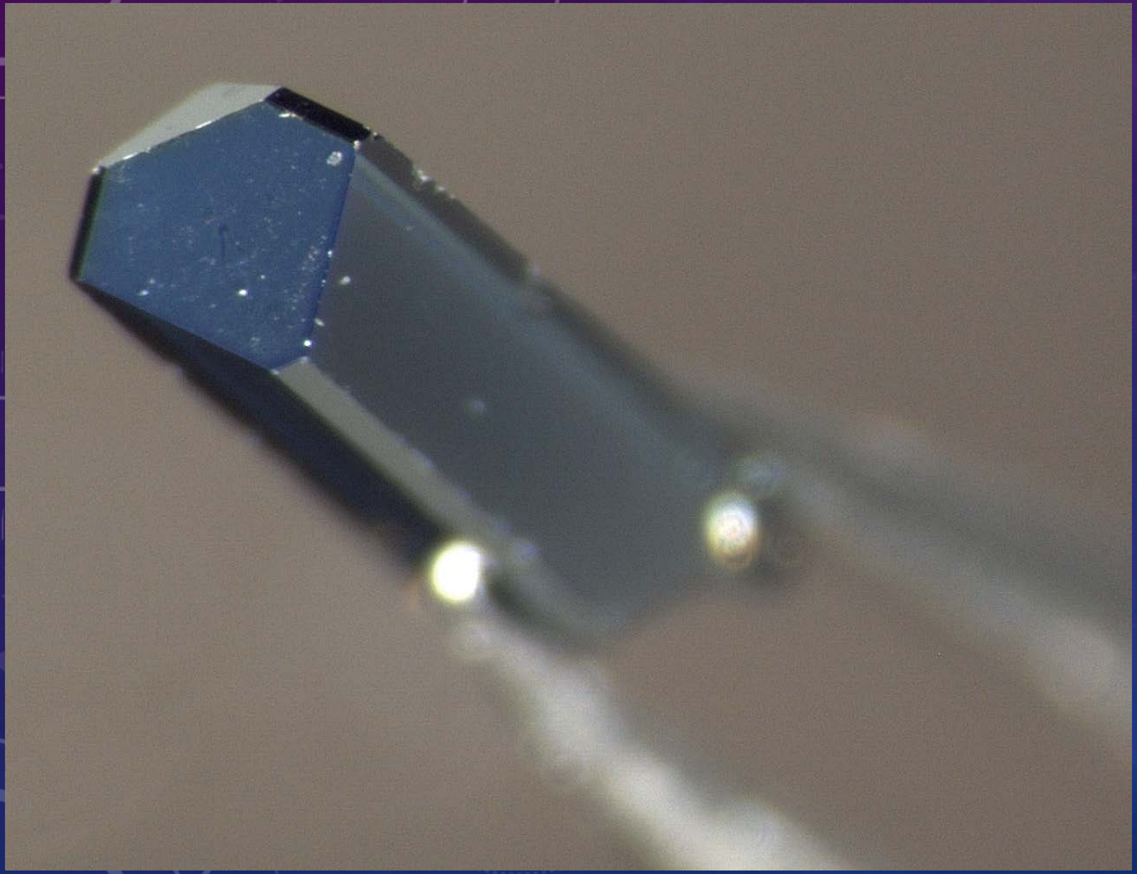

$Cu_2ZnSiSe_4$ single crystal

- wide gap chalcogenides
- ternary nitrides
- hybride halide perovskites
- Inorganic halide perovskites
- chalcogenide perovskites
- chalcohalides

→ powder, single crystals, polycrstalline thin films

Useful defects

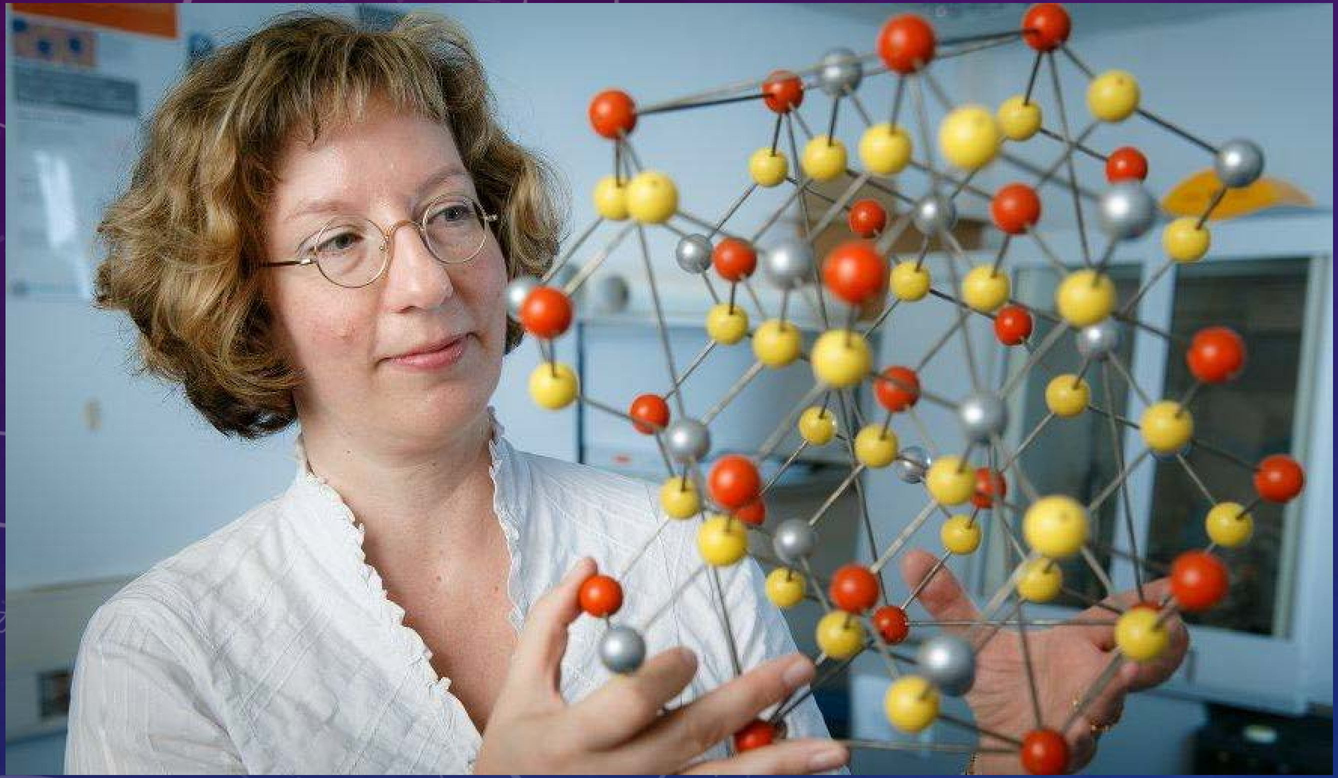

- one focus of our research is on structural disorder, particularly on point defects
- these defects have a major influence on the properties and efficiency of a thin-film solar cell

Advanced analytic for optoelectronic properties

Thomas Unold discussing in the thin film lab

- **decay kinetics from TRPL, pump-probe Thz spectroscopy**
- **doping density from Kelvin Probe, CV, TRPL**
- **quasi-Fermi Level Splitting from hyperspectral PL Imaging**
- **custom functional layers from Pulsed Laser Deposition (PLD) to grow materials libraries**

→ combinatorial high-throughput materials optimization

Education of young scientists

PhD student Elisa Valle Rios at the Electron Microprobe

- teaching at the Freie Universitaet Berlin
- teaching at international schools
  - NEXTGENPV School
  - Roentgen-Angstroem Cluster School
  - ANSTO Neutron Training Course
- organize and teach the X-ray Diffraction School and the Rietveld School at HZB‘s X-Ray CoreLab (for PhD students)
- supervision of MSc student
- supervision of PhD students

Galina Gurieva teaching in a high school seminar

Department Structure and Dynamics of Energy Materials

Head of department: Prof. Dr. Susan Schorr

Professor at the Freien Universität Berlin, Institute of Geological Sciences

Crystallographic materials research

Group leader:
Dr. Galina Gurieva

Combinatorial Materials Research & spectroscopy

Group leader:
Dr. Thomas Unold

Correlative Electron Microscopy

Group leader:
Dr. Daniel Abou-Ras

Diffraction and spectroscopy with synchrotron radiation

Group leader:
Dr. Daniel Többens

our aim … **investigation of structure – property – function relationships of compound semiconductors for solar energy conversion**

we run the X-Ray CoreLab, a central facility of HZB

… about 27 scientists, PhD students, technicians

What is structural disorder?

crystalline material … 3-dimensional periodic arrangement of atoms/ions/…

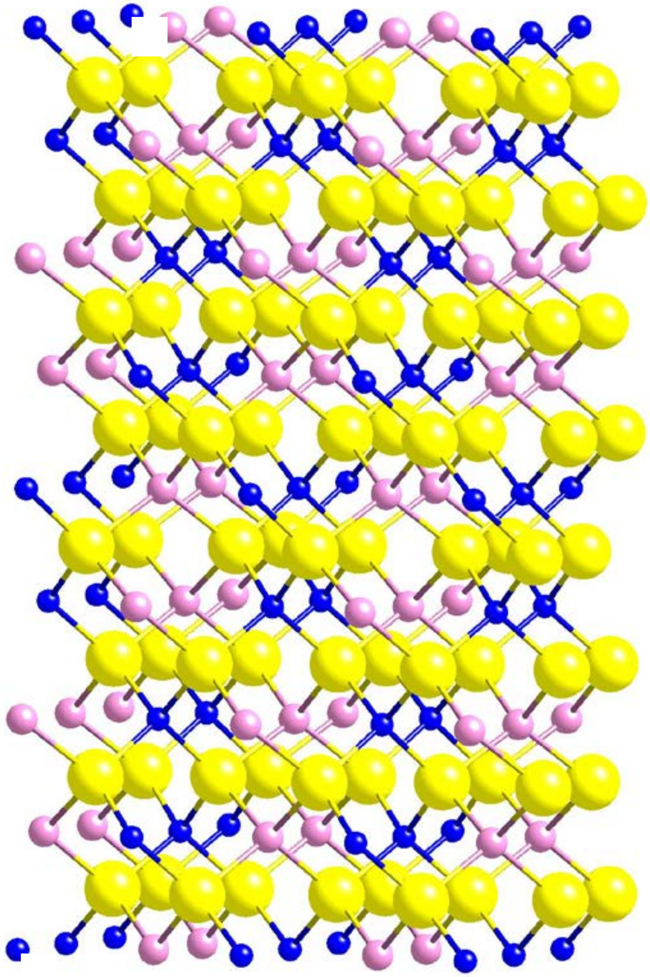

But this is the ideal world!

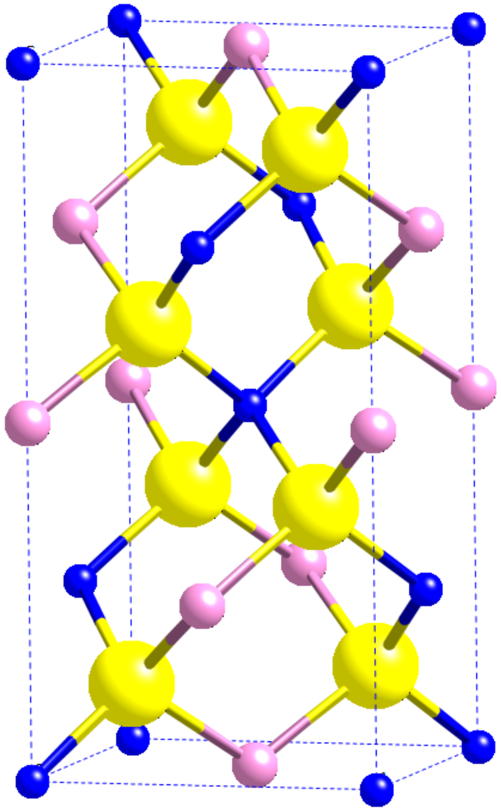

… in the real world ➞ defects ➞ real structure

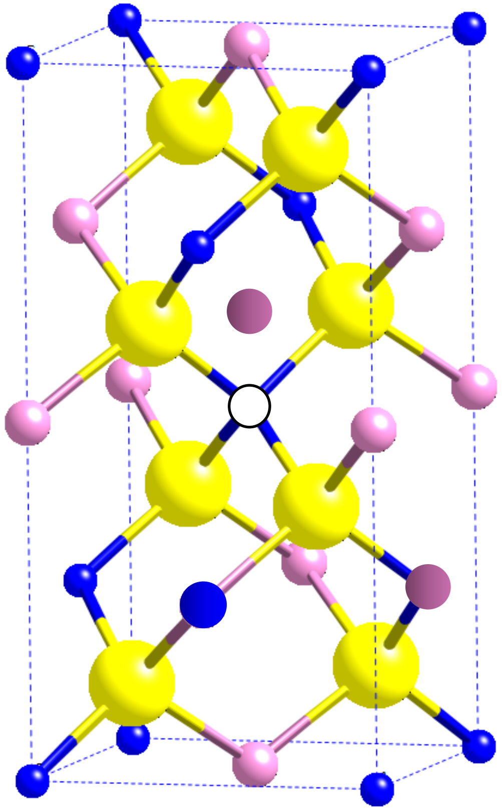

structural disorder

interstitials

vacancies

anti-sites

$\underbrace{\hspace{6em}}$

point defects

Why structural disorder is important?

The properties of crystalline semiconductors are mainly due to the presence of *defects inside the crystal structure*.

Managing their influence on electronic properties is critical for high performance across a range of technologies, including PV.

Of particular importance are point defects.

First of all we have to understand them – their structural origin, their concentrations and how this depends on chemical composition etc.

Defects play a crucial role

$Cu(In,Ga)Se_2$

„Chalcopyrites“

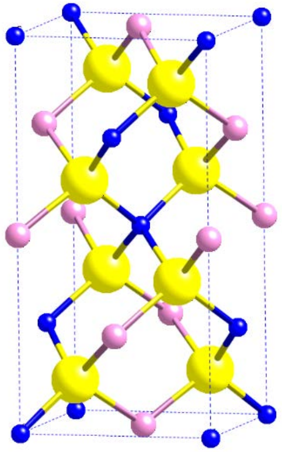

Chalcopyrite type
crystal structure

$Cu_2Zn(Ge,Sn)(S,Se)_4$

„Kesterites“

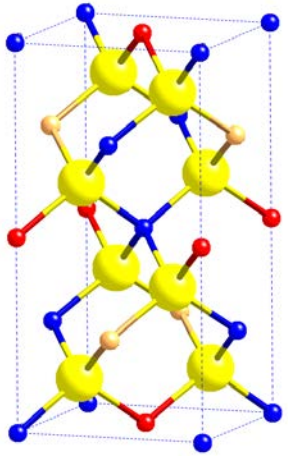

Kesterite type
crystal structure

copper vacancies (V_{Cu})
→ dominant intrinsic defect
→ causes p-type conductivity
→ shallow acceptor

complex point defect scenario

shallow defects → low SRH rates → beningn → „good“ defect
deep defects → high SRH rates → detrimental → „bad“ defect

→ intrinsic semiconductors

→ intrinsically doped by point defects

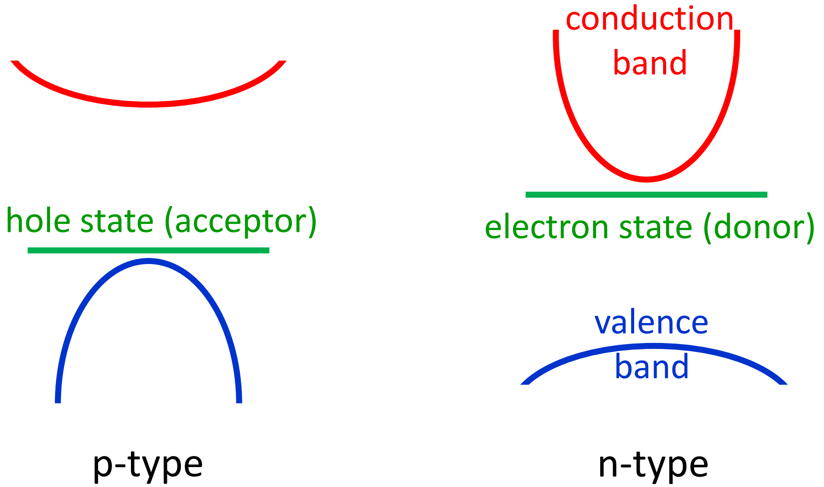

- alteration of optoelectronic properties p – type/n – type conductivity
- defects introduce energy levels (traps) in the band gap → annihilate charge carriers (Shockley-Read-Hall recombination-SRH)
- deep defects act as recombination centers

Structural perception of intrinsic point defects

defect levels obtained by spectroscopy (e. g. PL)

BUT: very little evidence exists as to the **chemical and structural identification of the defect** producing those levels

crystal structure analysis by X-ray diffraction **and neutron diffraction**

$\Rightarrow$ **point defects change significantly the scattering cross section σ_{coh} of the cation structural sites**

scattering cross section σ_{scat} is a hypothetical area which describes the likelihood of X-rays / neutrons being scattered by an atom / nucleous

$Cu(In,Ga)S_2$ $Cu(In,Ga)Se_2$

Cu_2ZnSnS_4 $Cu_2ZnSnSe_4$

Cu_2ZnGeS_4 $Cu_2ZnGeSe_4$

$ZnGeN_2$

BUT: Cu, Zn, Ga and Ge are electronic similar elements

Cu^+, Zn^{2+}, Ga^{3+} and Ge^{4+} are isoelectronic → equal atomic scattering factor f

X-ray diffraction

$$\sigma_{coh} \sim f^2$$

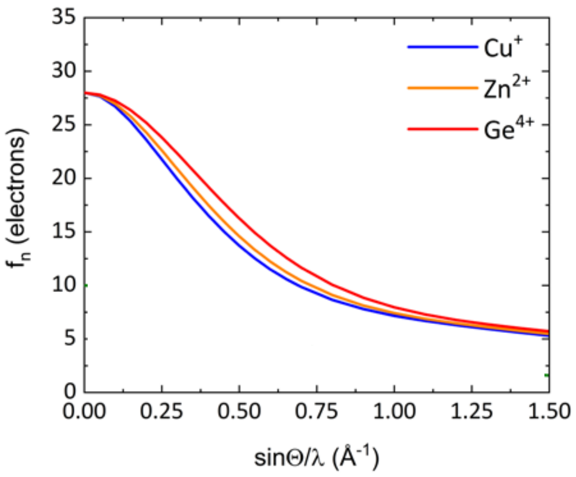

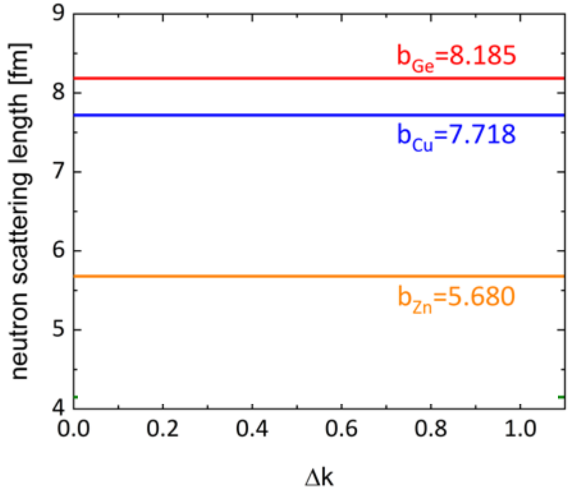

neutron diffraction

$$\sigma_{coh} \sim b^2$$

Average neutron scattering analysis method

Kesterite type structure

(space group $I\bar{4}$)

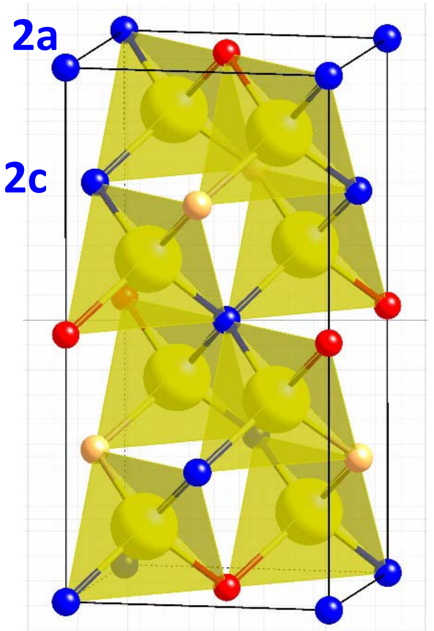

Cu_{Zn}
Zn_{Cu}
Zn_{Sn}
Cu_{Sn}
Sn_{Cu}
Sn_{Zn}
V_{Cu}
V_{Zn}
V_{Sn}
Cu_i
Zn_i
Sn_i

4 cation sites

2a … occupied by **Cu**
2c … occupied by **Cu**
2d … occupied by **Zn**
2b … occupied by **Sn**

cation site occupancy factor (SOF)

from Rietveld analysis of

neutron diffraction data

neutron scattering lengths

Cu: 7.718 fm

Zn: 5.680 fm

Sn: 6.225 fm

Ge: 8.185 fm

experimental average neutron scattering length

$$\bar{b}_{2a}(\exp) = SOF_{2a} \cdot b_{Cu}$$
$$\bar{b}_{2c}(\exp) = SOF_{2c} \cdot b_{Cu}$$
$$\bar{b}_{2d}(\exp) = SOF_{2d} \cdot b_{Zn}$$
$$\bar{b}_{2b}(\exp) = SOF_{2b} \cdot b_{Sn}$$

calculated average neutron scattering length → cation distribution model based on off-stoichiometry types

$$\bar{b}_j(calc) = \sum_k (k)_j^{model} \cdot b_k$$

j=2a, 2c, 2d, 2b
k=Cu,Zn, IV

$(k)_j^{model}$ - *fraction of cation k on site j*

additional requirements:

(1) each cation site is fully occupied

$$(k)_j^{model} + V_k^{model} = 1$$

j=2a, 2c, 2d, 2b
k=Cu,Zn,IV (Sn,Ge)
V - vacancy

(2) the sum of a cation species in the model is the cation species amount measured by WDX

$$\sum_j (k)^{model} = k^{WDX}$$

S. R. Hall et al., Can. Mineral. 16 (1978) 131

Schorr et al. in: Advanced characterization techniques for thin film solar cells, Wiley, 2016

Experimental determination of intrinsic point defects (type & concentr.)

Average neutron scattering length analysis method

Schorr et al. in: Advanced characterization techniques for thin film solar cells, Wiley, 2016

pre-requesit → determination of **chemical composition** of quaternary phase by **WDX** spectroscopy
→ homogeneous powder sample

neutron diffraction

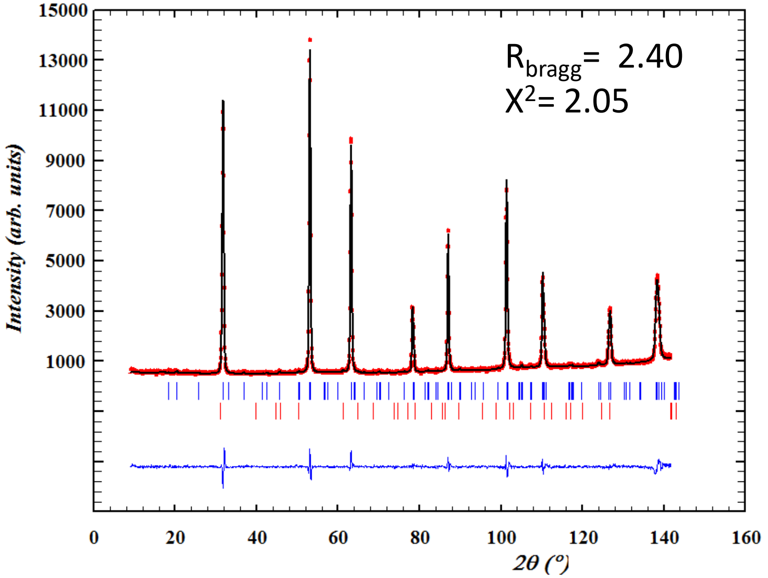

average neutron scattering lengths

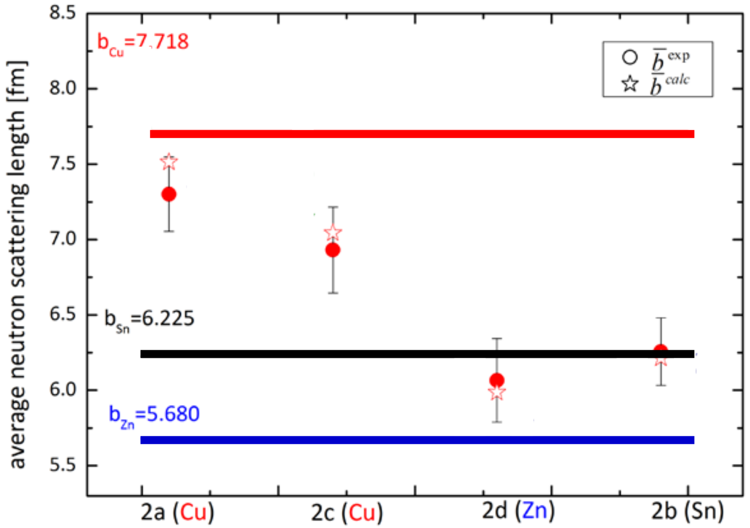

cation distribution model

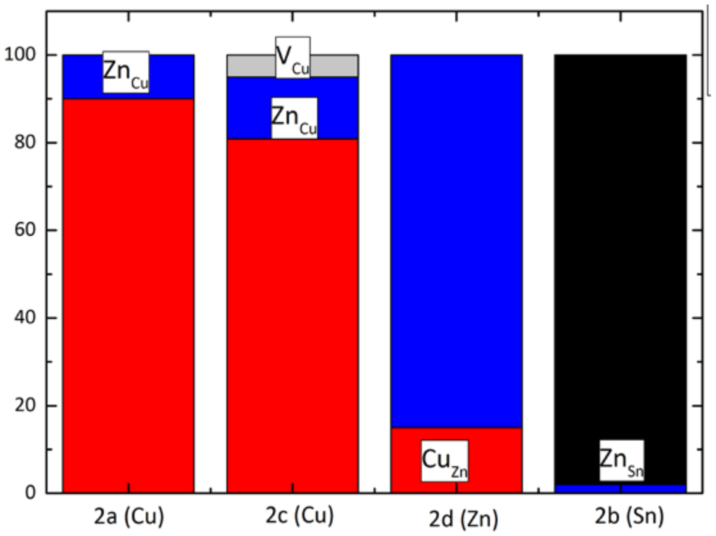

simultaneous Rietveld analysis of diffraction data (X-ray & neutron)

site occupancy factors (SOF)

average neutron scattering length analysis

minimizing the difference between $\bar{b}^{exp}$ and $\bar{b}^{calc}$ by varying the cation distribution

intrinsic point defects

- type
- concentration (quantitative!)

Our experimental strategy: systematic investigation of materials properties

HZB Helmholtz Zentrum Berlin

synthesis of powder samples

solid state reaction of the elements in closed silica tubes (750 – 950°C)

reacted elements

pellet

chemical analysis

WDX spectroscopy
(calibrated system using standards)

BSE picture

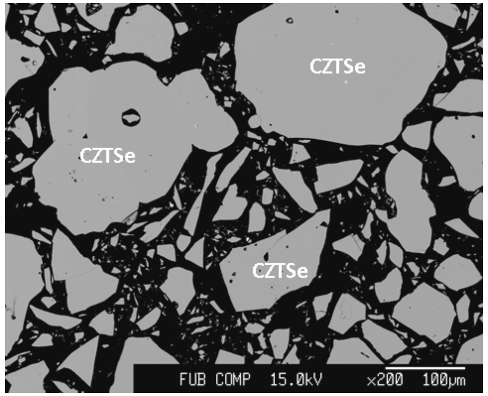

grey – grains
black - epoxy

X-ray diffraction

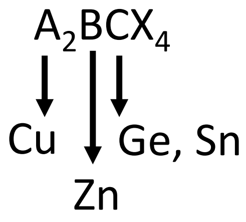

A_2BCX_4

Cu

Zn

Ge, Sn

Cu^+, Zn^{2+} and Ge^{4+} are isoelectronic
→ very similar atomic form factor *f*

neutron diffraction

experiments performed at neutron sources all over the world

Rietveld analysis of powder diffraction data

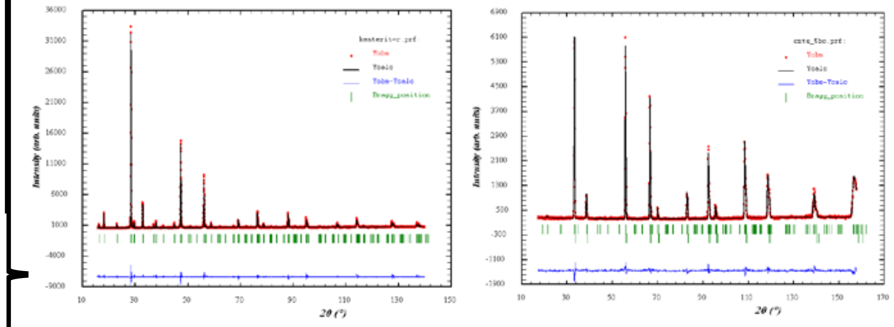

X-ray diffraction

neutron diffraction

determination of

- structural parameters, SOFs
- cation distribution
- cation point defect concentration

UV-ViS spectroscopy

- measurements of diffuse reflectance
- Kubelka–Munk pseudo-absorption function $F(R) = \frac{(1-R)^2}{2R}$
- Tauc plot → plotting $(F(R)*h\nu)^2$ versus photon energy $h\nu$ → derive E_g

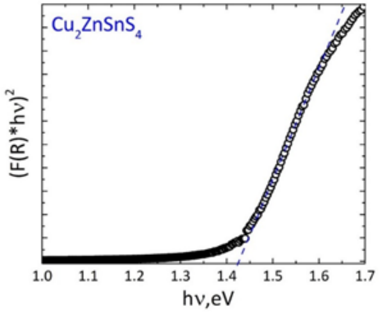

(i) Cu-Zn disorder in kesterite-type materials

(ii) off-stoichiometry in kesterite-type materials

(iii) off-stoichiometry in quaternary chalcogenides – „kesterite-derived“ materials

(iv) structural disorder in ternary nitrides

(v) Structural disorder hybrid halide perovskites?

Cu/Zn disorder in kesterite-type materials: discovered by neutron diffraction

„ideal“ Kesterite

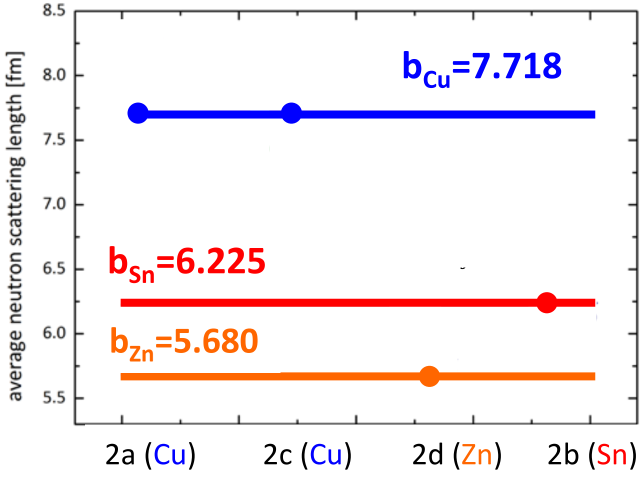

„real“ Kesterite

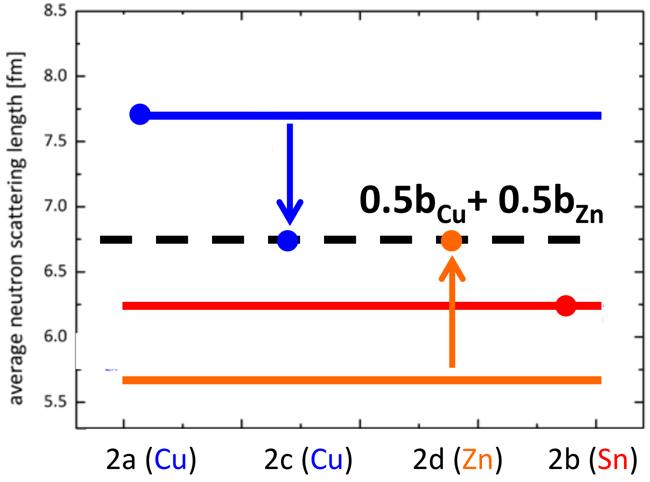

cation distribution model

cation order

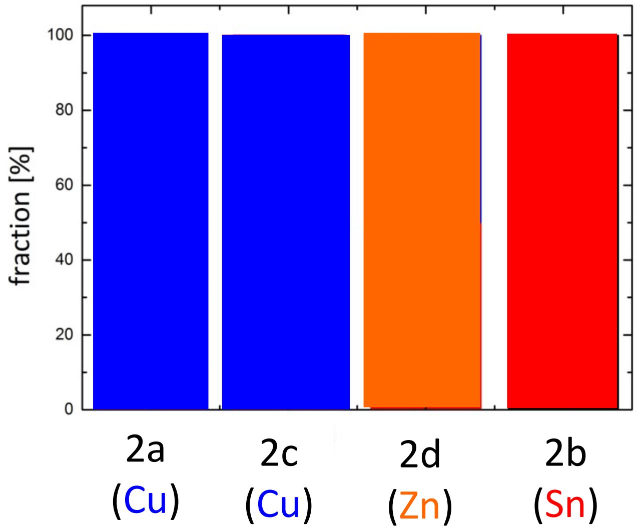

Cu – Zn disorder

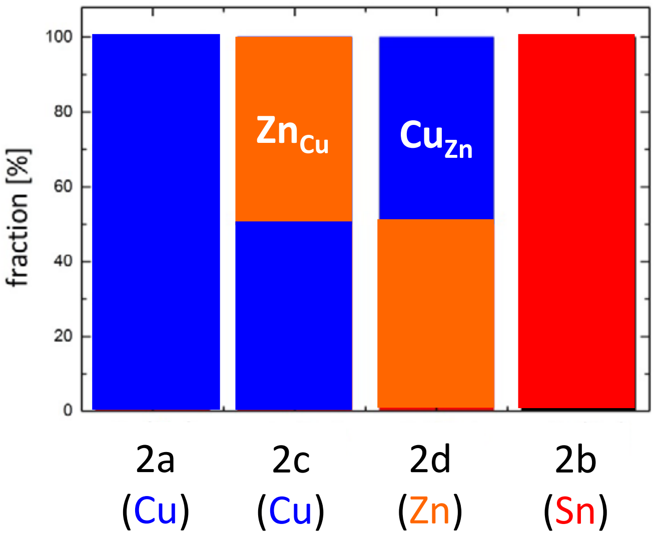

Wyckoff position

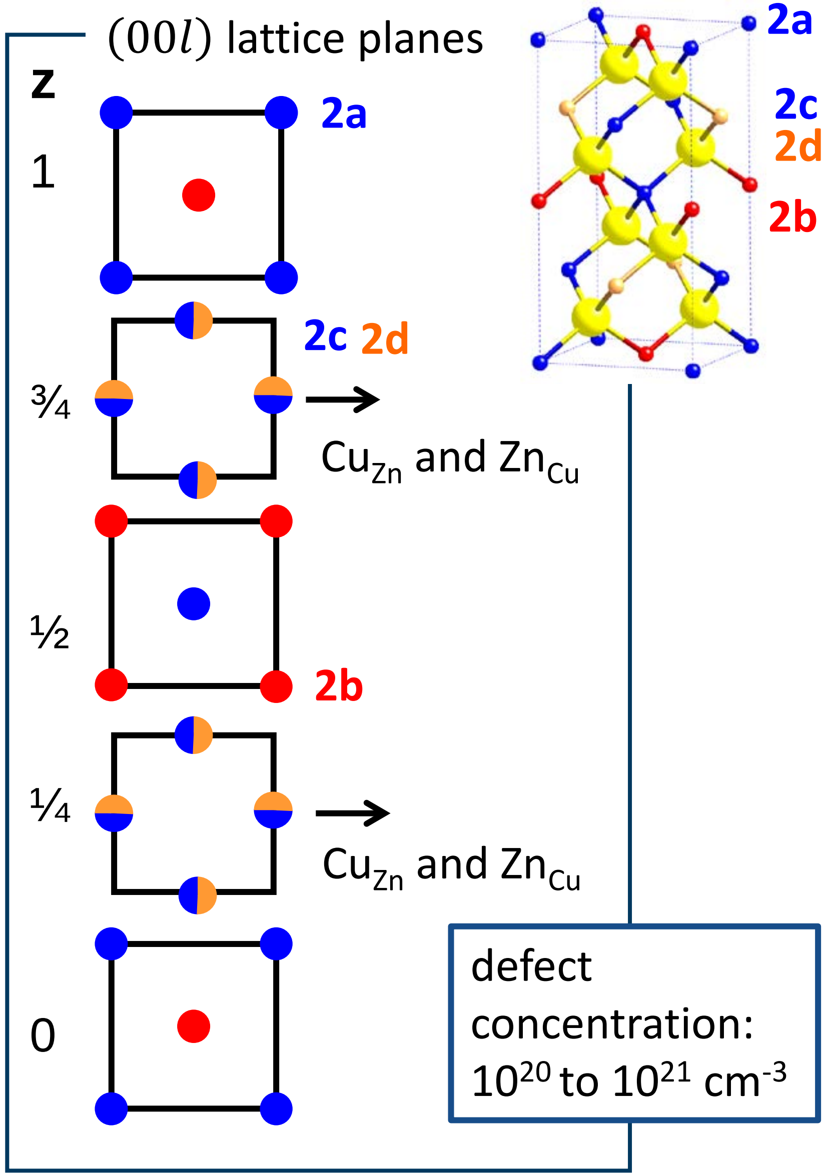

defect concentration: 10^{20} to 10^{21} cm^{-3}

Schorr et al., Europ. J. Mineral. 19 (2007) 65

The Cu/Zn order – disorder phase transition

Lattice parameter obtained by *in-situ* synchrotron X-ray diffraction (ESRF)
→ first hint for a change in cation distribution

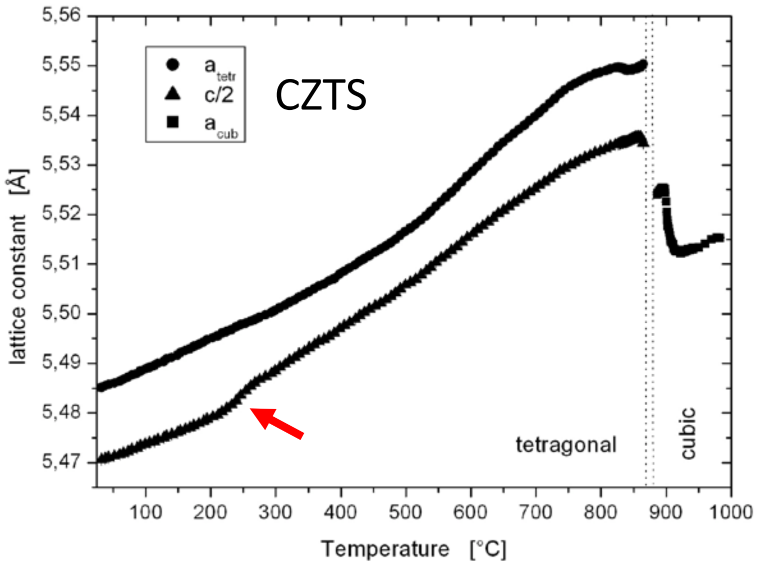

T_C (CZTS) ≅ 240 – 260 °C

S. Schorr et al., Phys Stat Sol A 206 (2009) 1054

order-disorder transition described qualitatively by
the **ratio of two Raman peaks**

$$Q = I(m_{2A})/I(m_{3A})$$

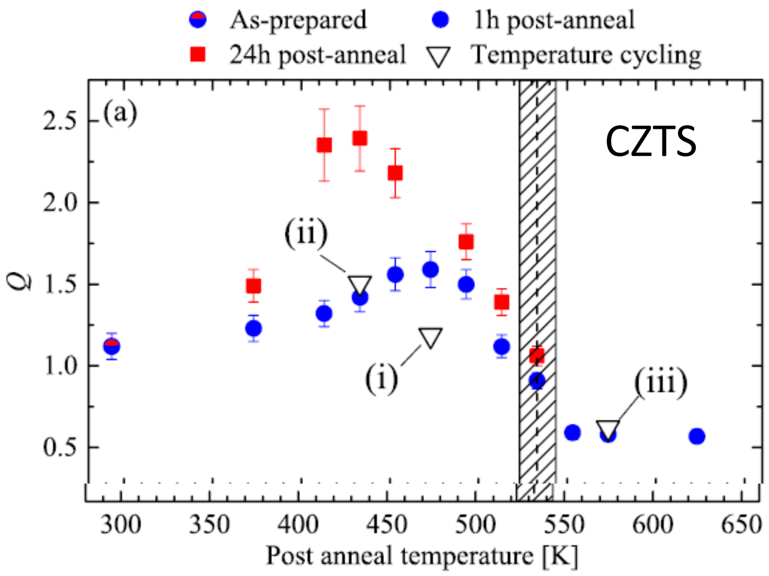

T_C(CTZS) ≅ 260°C

J. Scragg et al., APL 104 (2014) 041911

order-disorder transition described quantitatively by
the site occupancy of 2c and 2d sites

$$Q = \frac{[Cu_{2c} + Zn_{2d}] - [Zn_{2c} + Cu_{2d}]}{[Cu_{2c} + Zn_{2d}] + [Zn_{2c} + Cu_{2d}]}$$

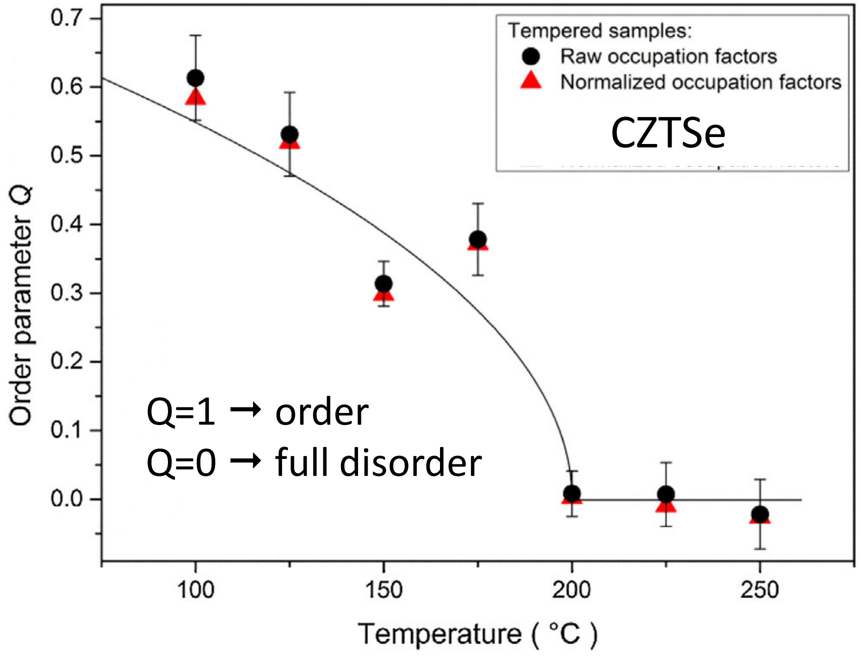

Q=1 → order
Q=0 → full disorder

T_C(CTZSe) ≅ 190°C

D.M. Többens et al., Phys Stat Sol B 253 (2016) 1890

Correlation of Cu/Zn disorder and optoelectronic properties

UV-Vis spectroscopy

➞ band gap energy E_g increases with decreasing disorder

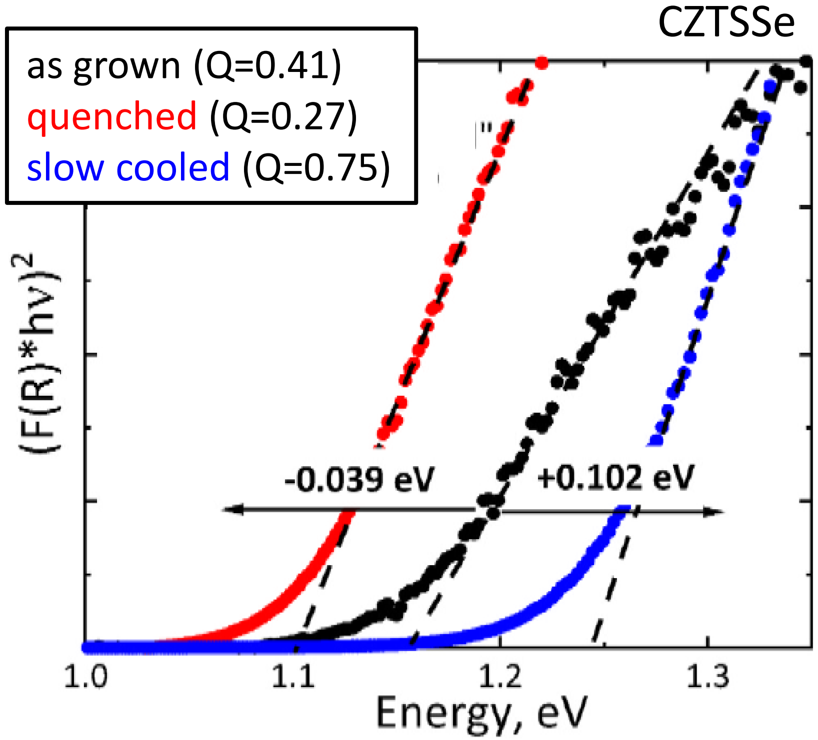

Gurieva et al., Sol. En. Mat. Sol. Cells 248 (2022) 112009

Photoluminescence

➞ PL_{max} increases with decreasing disorder

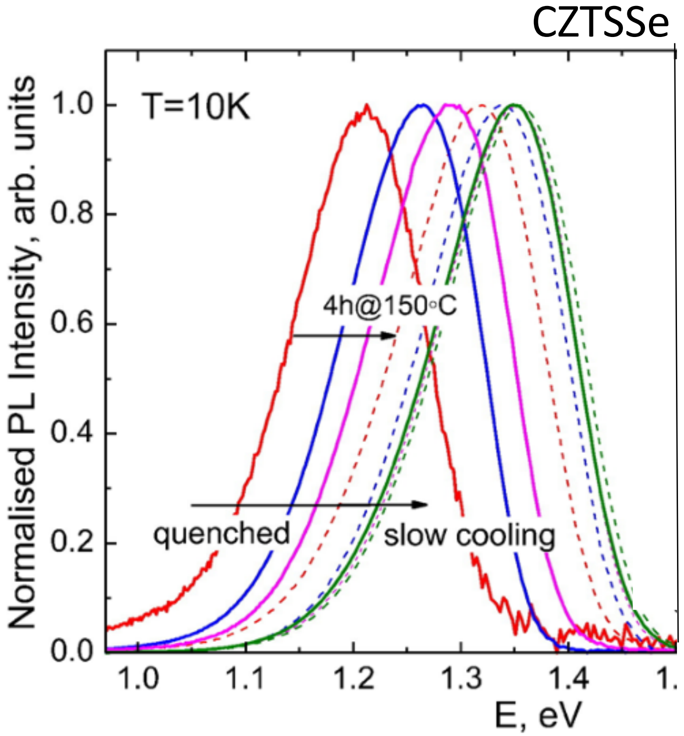

Annealing below the order-disorder transition temperature

➞ decrease of Cu/Zn disorder

➞ increase of V_{OC}

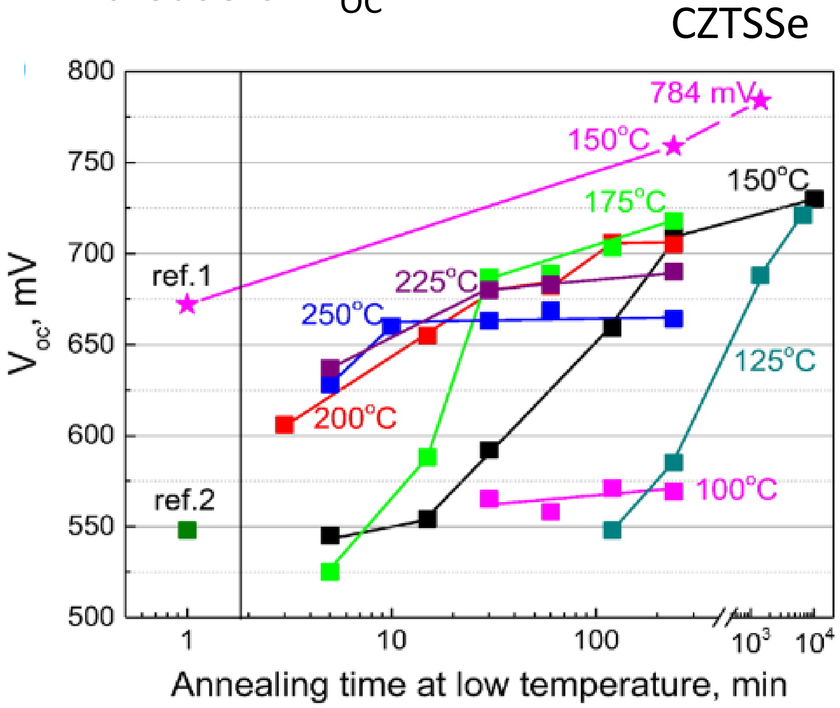

Li et al., npj Flexible Electronics 16 (2023)

Technology development: low temperature annealing ($T < T_C$) as post-deposition treatment of the solar absorber ➞ decrease of Cu/Zn disorder

Is there a possibility to avoid Cu/Zn disorder?

average neutron scattering length analysis

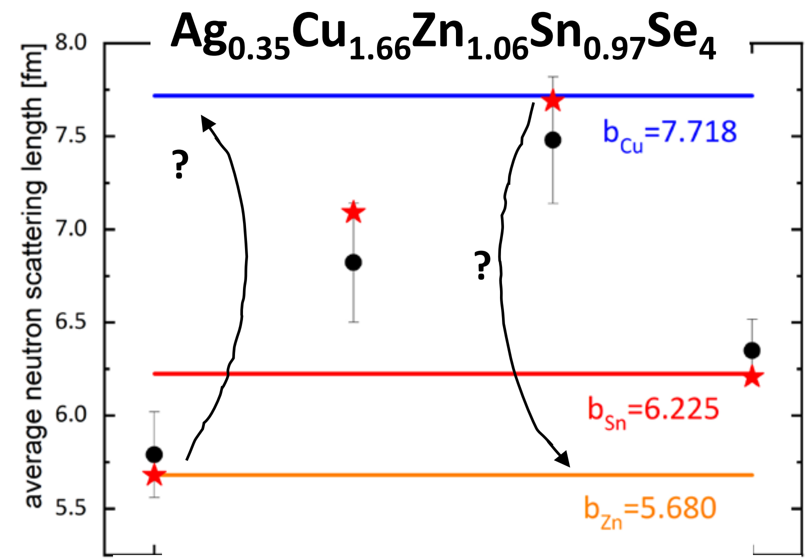

cation distribution model

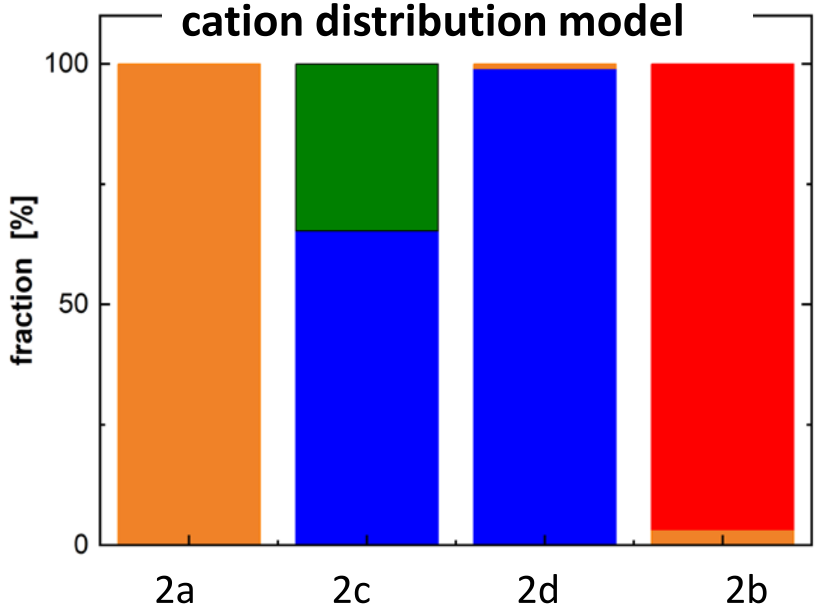

derived crystal structure

→ **Stannite-type structure**

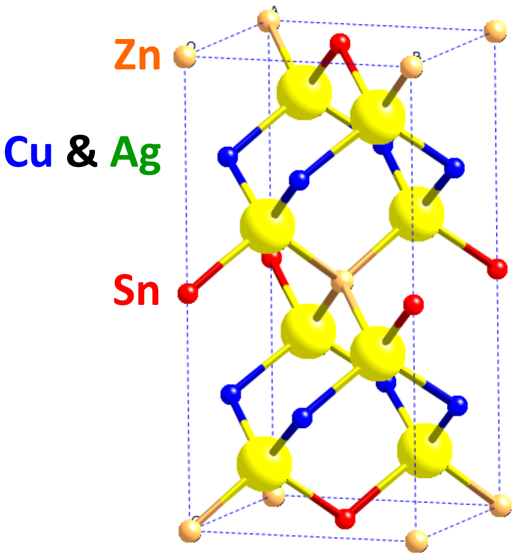

substituting Cu by Ag

→ change to Stannite structure

→ no Cu/Zn disorder

significant increase in Q_e^{PL}

→ due to a strongly increased SRH lifetime caused by a **reduction in non-radiative recombination via defects**

band gap energy in $(Ag,Cu)ZnSnSe_4$

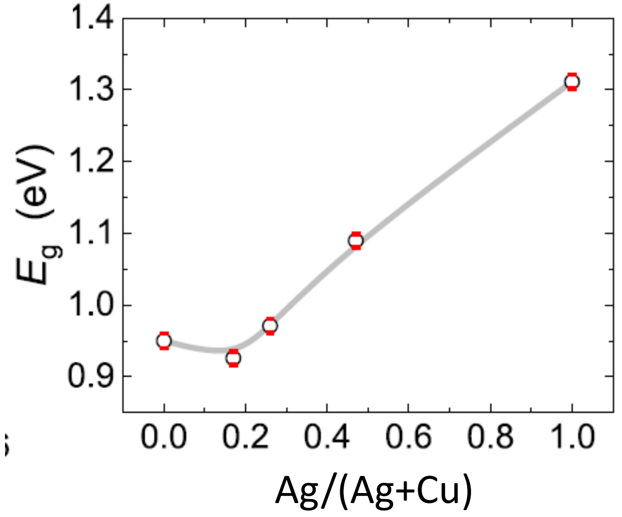

external quantum yield Q_e^{PL}

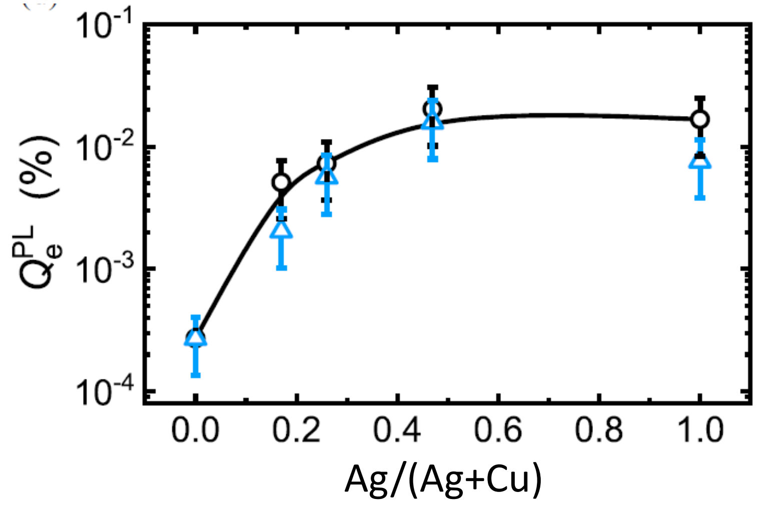

G. Gurieva et al., Phys.Rev. Mat. 4 (2020) 054602

(i) Cu-Zn disorder in kesterite-type materials

(ii) off-stoichiometry in kesterite-type materials

(iii) off-stoichiometry in quaternary chalcogenides – „kesterite-derived“ materials

(iv) structural disorder in ternary nitrides

(v) Structural disorder hybrid halide perovskites?

Off-stoichiometry in the kesterite absorber layer

highest efficiency in CZTS,Se-based solar cells
→ Cu-poor/Zn-rich composition

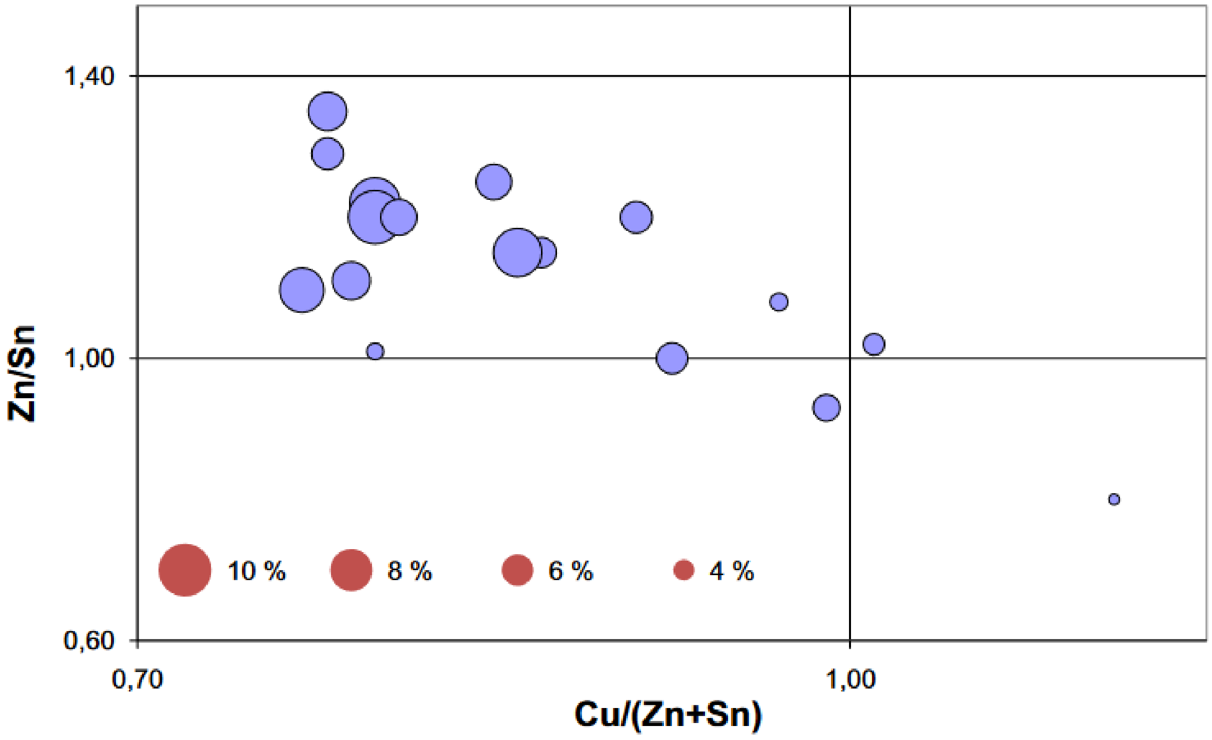

Delbos, *EPJ Photovoltaics 3 (2012) 35004*

Physica Status Solidi a 215 (2018) 1700957


ORIGINAL PAPER

Off-Stoichiometry

www.pss-a.com

$Cu_2ZnSnSe_4$: How Far Does Off-Stoichiometry Go?

Galina Gurieva, Rafael Ferreira, Philipp Knoll, and Susan Schorr*

Model to describe off-stoichiometry

→ **off-stoichiometry type model**

correlates chemical composition and point defects

- off-stoichiometry types A, B, C, D

  *Lafond et al., Z. Anorg. Allg. Chem. 638 (**2012**) 2571*

- off-stoichiometry types E, F, G, H, I, J, K, L

  Gurieva et al., Journal fo Applied Physics 123 (2018) 161519

  Schorr et al., J. Physics: Energy 2 (2020) 012002

Flexibility of the crystal structure and off-stoichiometry

Kesterite-type structure is very flexible and can stabilize point defects (vacancies, anti sites, interstitials)

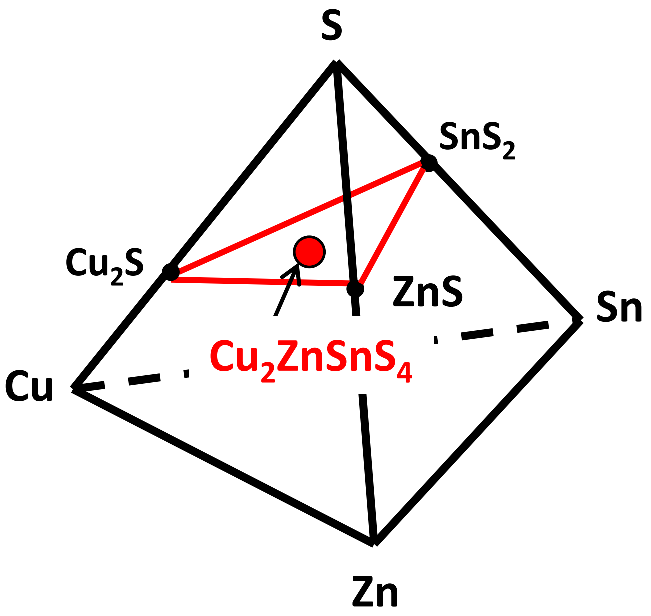

$Cu_2S – ZnS – SnS_2$

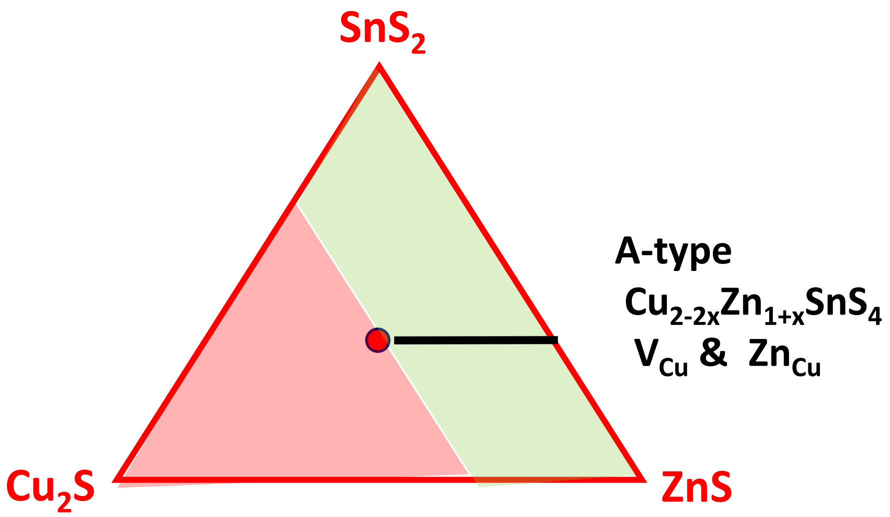

off-stoichiometry relations

Cu/(Zn + Sn) < 1	Zn/Sn > 1
Cu/(Zn + Sn) < 1	Zn/Sn < 1
Cu/(Zn + Sn) > 1	Zn/Sn > 1
Cu/(Zn + Sn) > 1	Zn/Sn < 1

off-stoichiometry type model (A-type … L-ype)

correlates off-stoichiometric composition and intrinsic point defects

→ defines existence regions for each point defect type

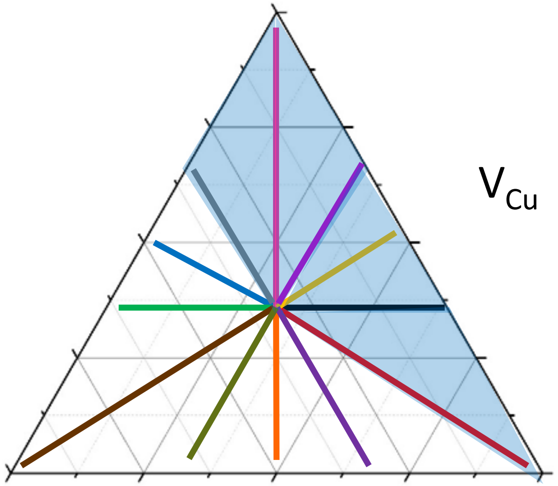

cation ratio plot

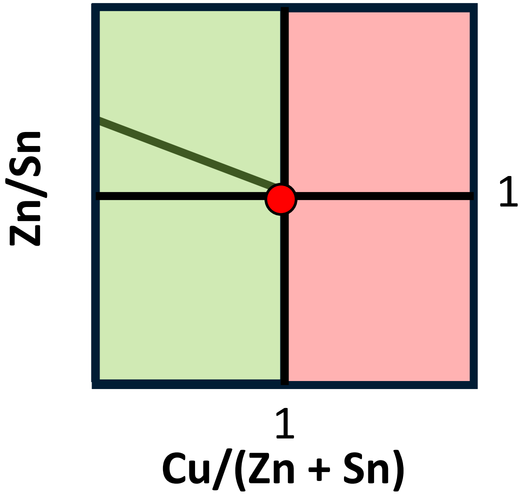

Gurieva et al., Journal of Applied Physics 123 (2018) 161519

Example: point defects in off-stoichiometric $Cu_2ZnGeSe_4$

cation ratio plot

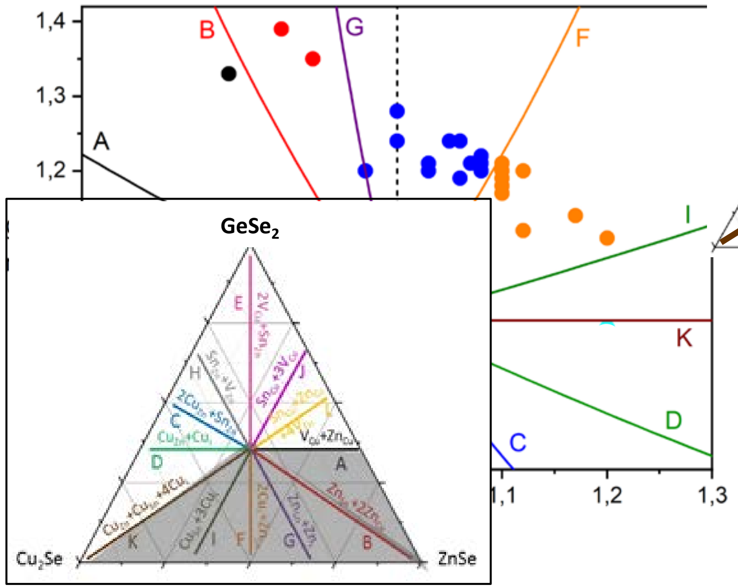

predicted intrinsic defects according to the off-stoichiometry type model

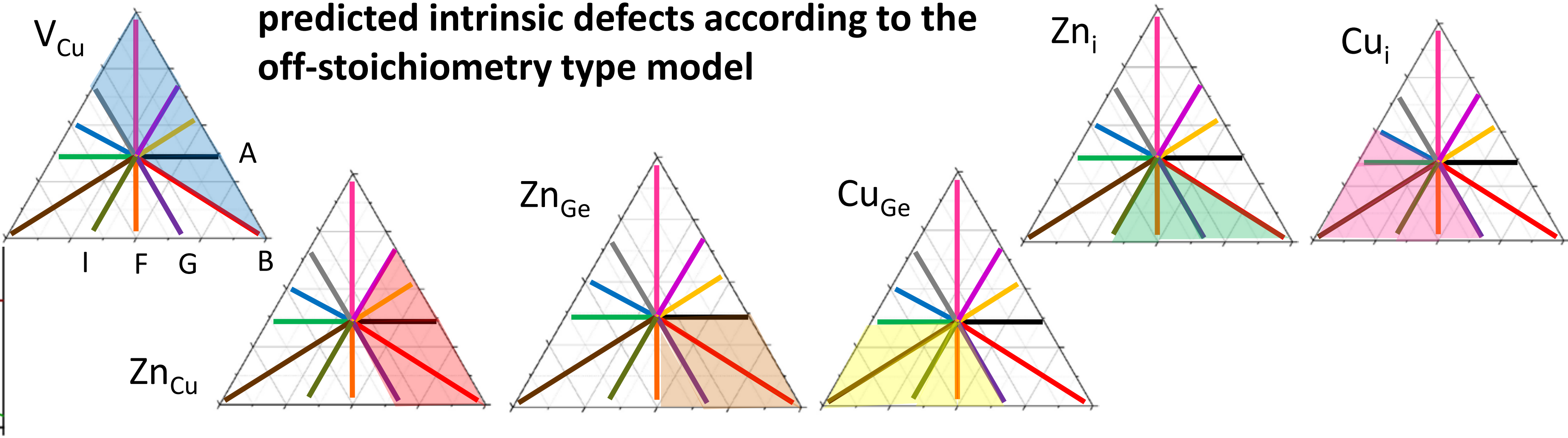

cation distribution resulting from neutron diffraction data analysis

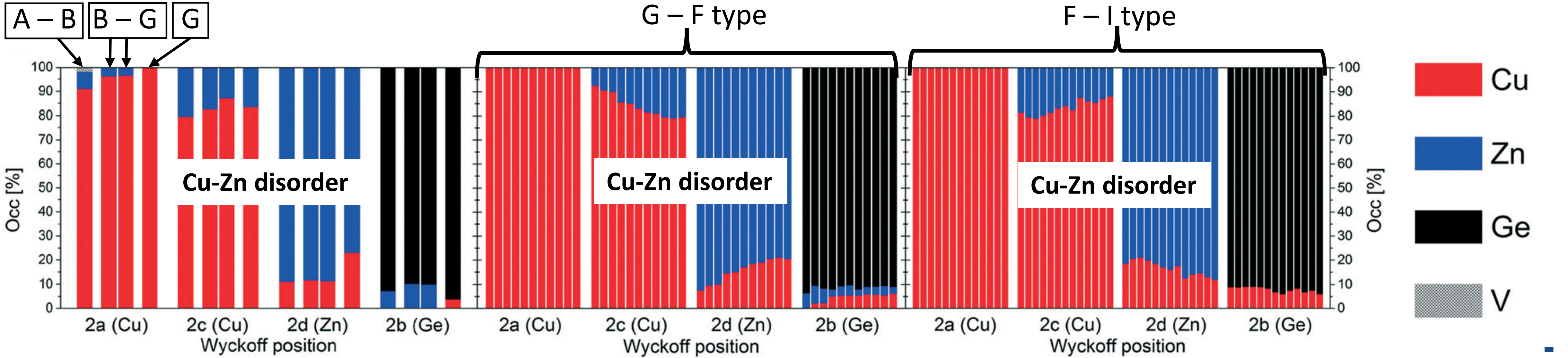

R. Gunder et al., Cryst. Eng. Comm 20 (2018) 1491 … cover picture!

Is there any „sweet“ spot for absorber composition?

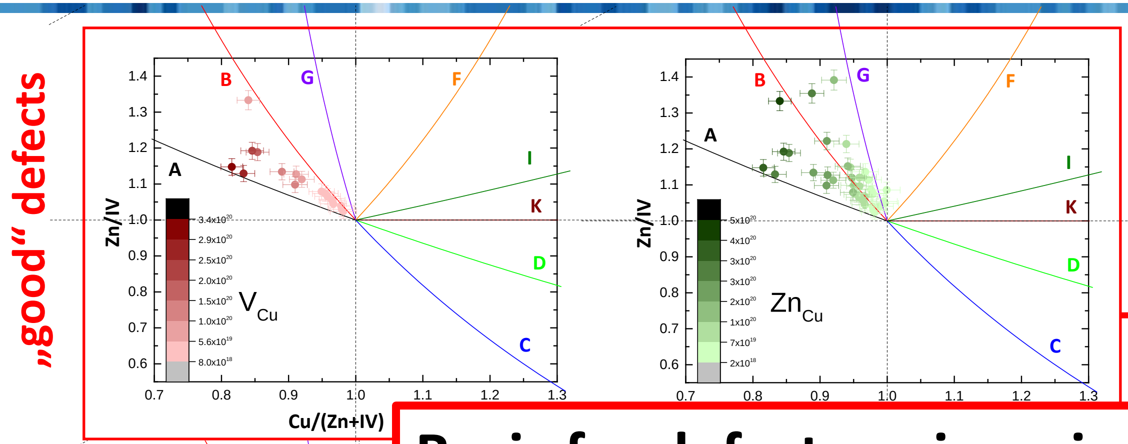
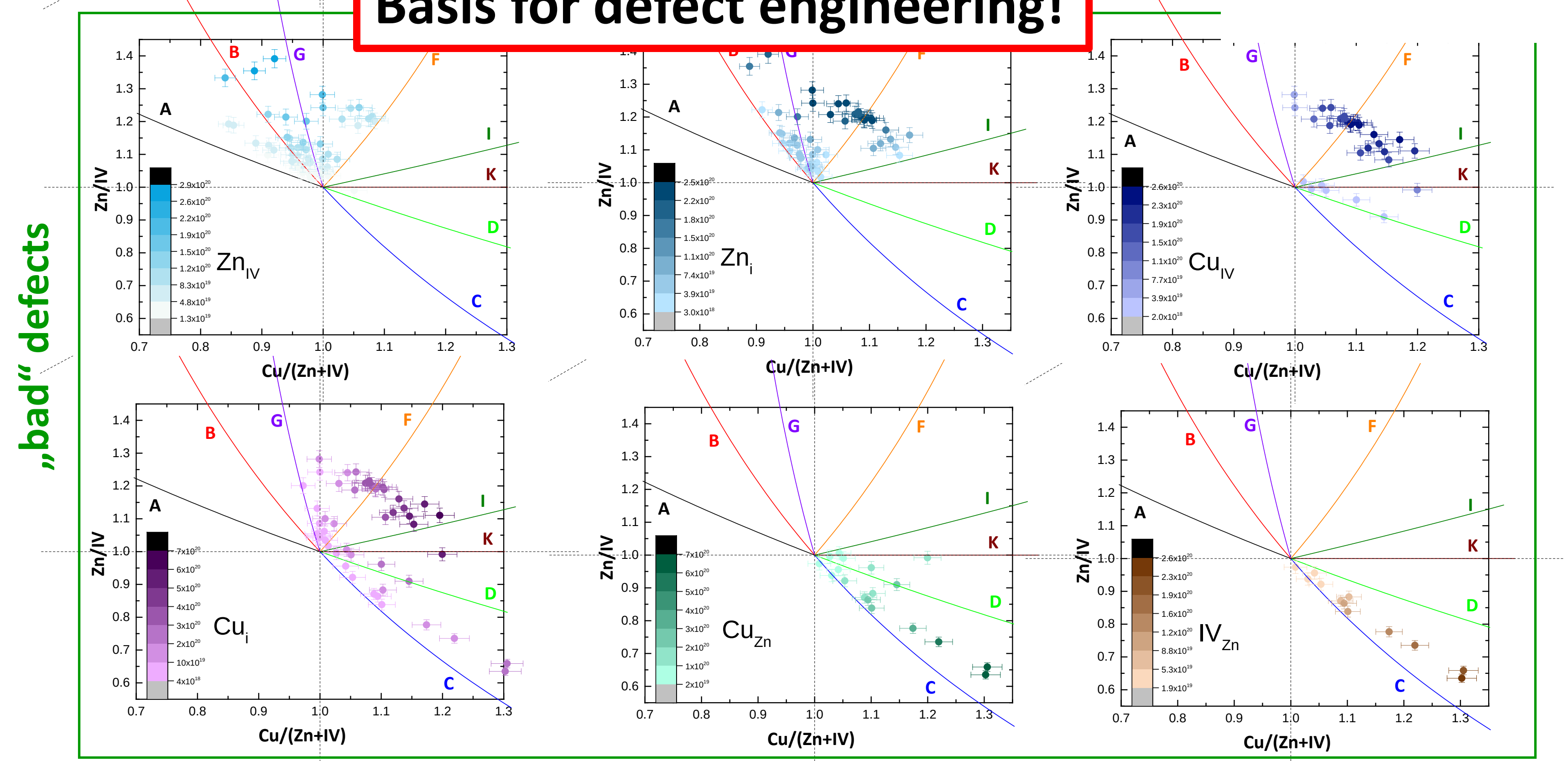

Basis for defect engineering!

favourable compositional region

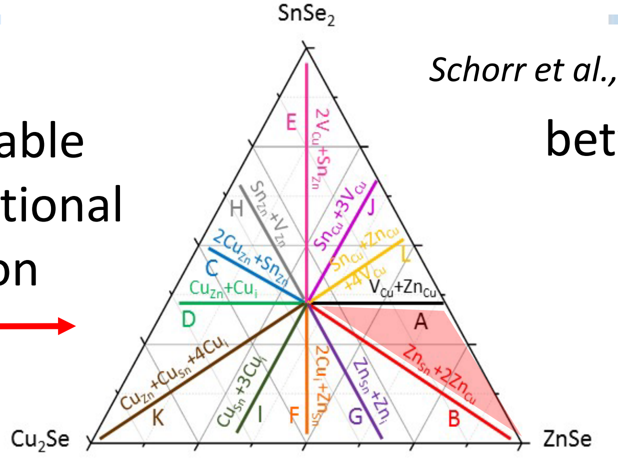

Schorr et al., J. Physics: Energy 2 (2020) 012002

between A - and B - type

V_{Cu}
Zn_{Cu}
Zn_{Sn}

CZTS

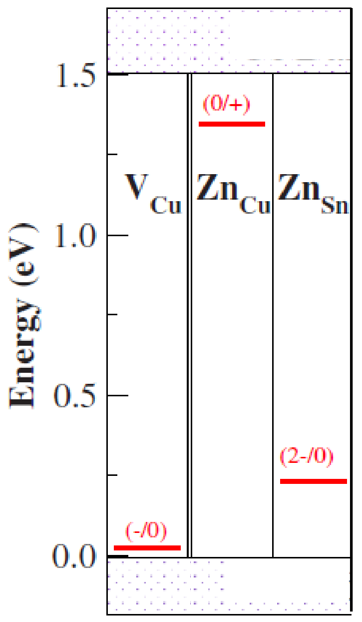

S. Chen et al, Phys. Rev. 81 (2010) 245204

Intrinsic point defects in kesterite-type solar absorbers

compositional variations of the absorber layer in the solar cell cause

→ variations in type and concentration of point defects

- **→ band gap fluctuations**
  - **→ electrostatic potential fluctuations → decrease V_{OC}**

E_g variations in CZTS

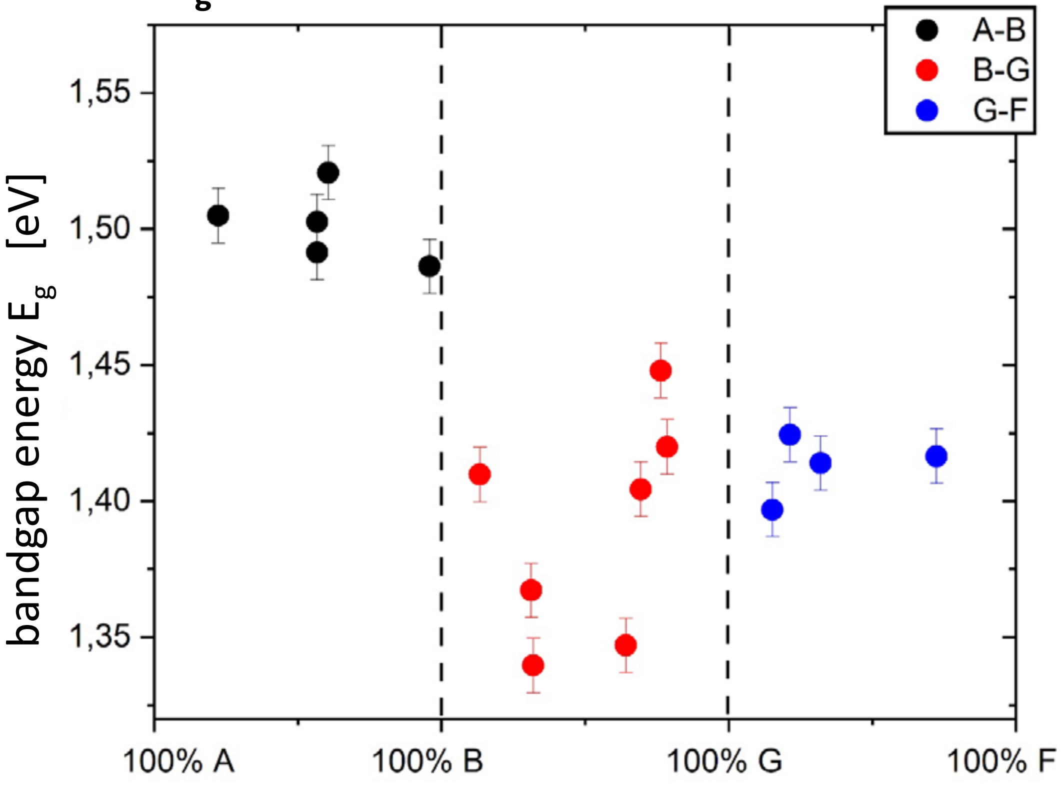

S. Schorr and C. Weidenthaler (Eds.), Crystallography in Materials Research, De Gruyter 2021

Optimisation of the absorber thin film growth process towards chemical homogeneity is crucial!

areal world example … composition of a CZTSe absorber layer (nanoXRF @ESRF)

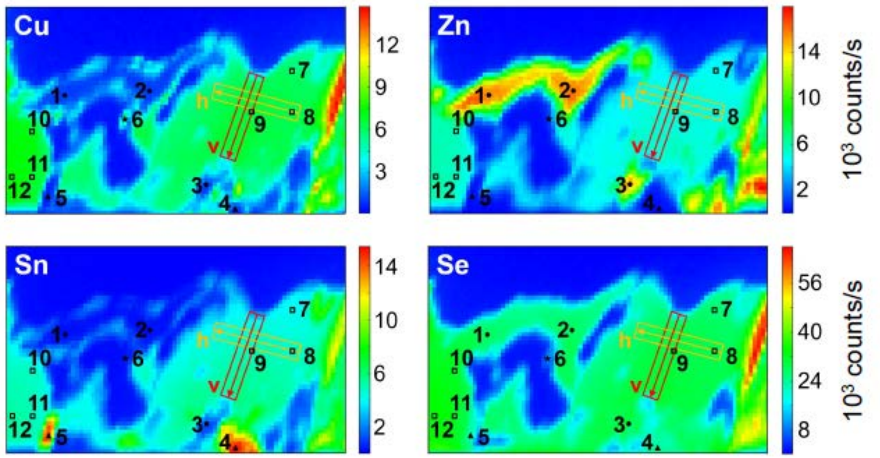

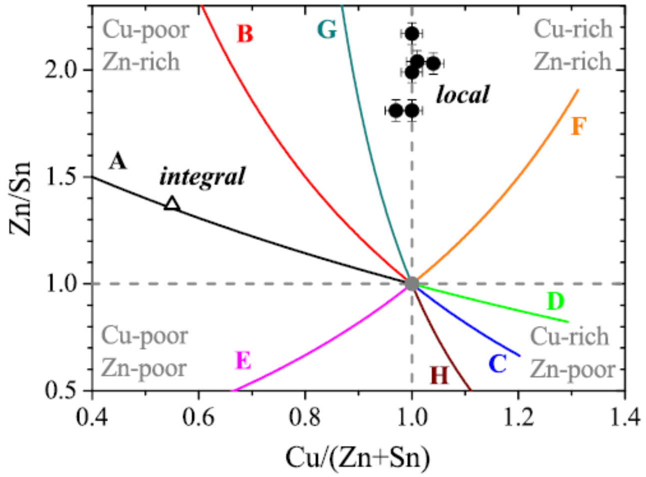

Schöppe, …, Saucedo, Schorr, Schnohr et al., Journal of Applied Physics 110 (2017) 043901

Monograin solar cells – correlate structural disorder and device parameter

Monograins → little single crystals

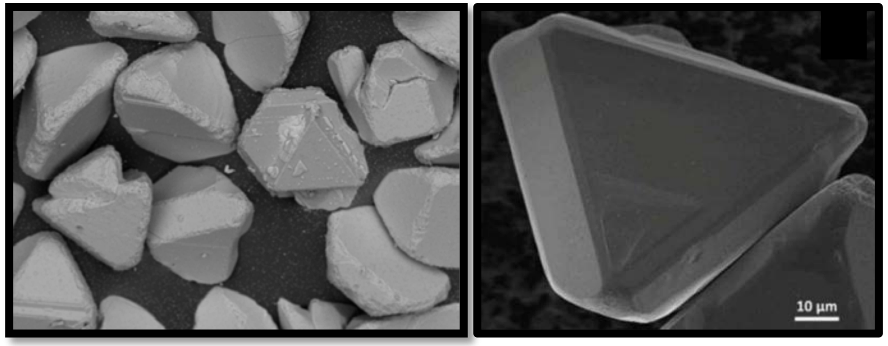

Monograin Solar Cell

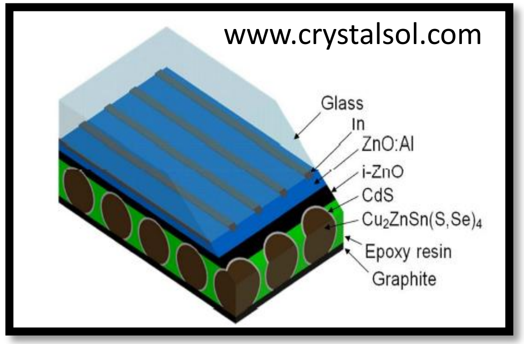

Monograins: Kesterite-type single crystals with homogenous chemical composition

suitable for neutron diffraction

→ enables determination of Q and point defects

working solar cell

→ device efficiency can be measured

correlation of structural disorder with PV parameters

CZTSSe monograins with S/(S+Se) = 0.6

Cu-Zn disorder (Q=1 … order)

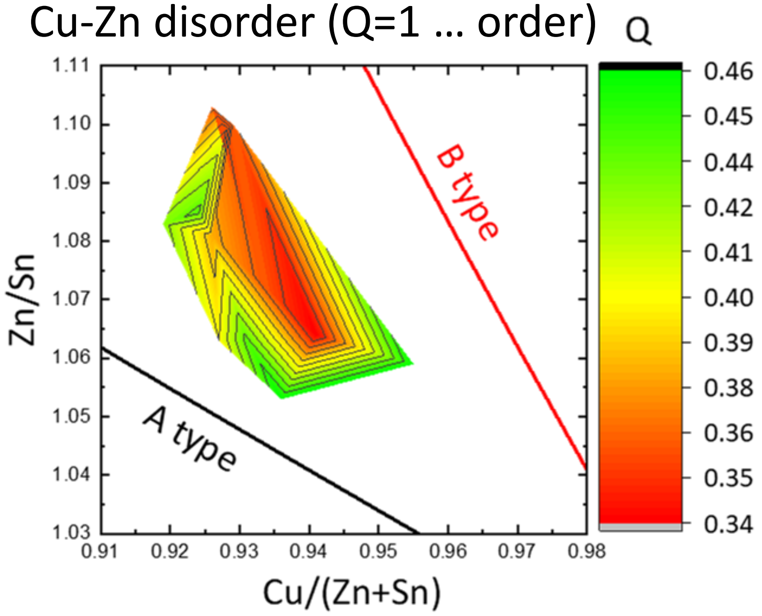

off-stoichiometry type related point defects: V_{Cu} Zn_{Cu} Zn_{Sn}

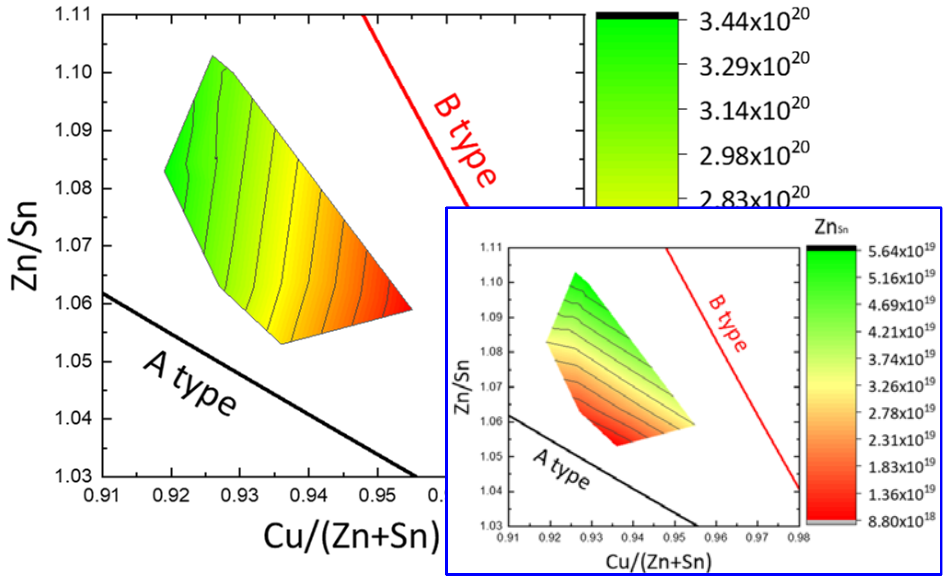

device efficiency (%)

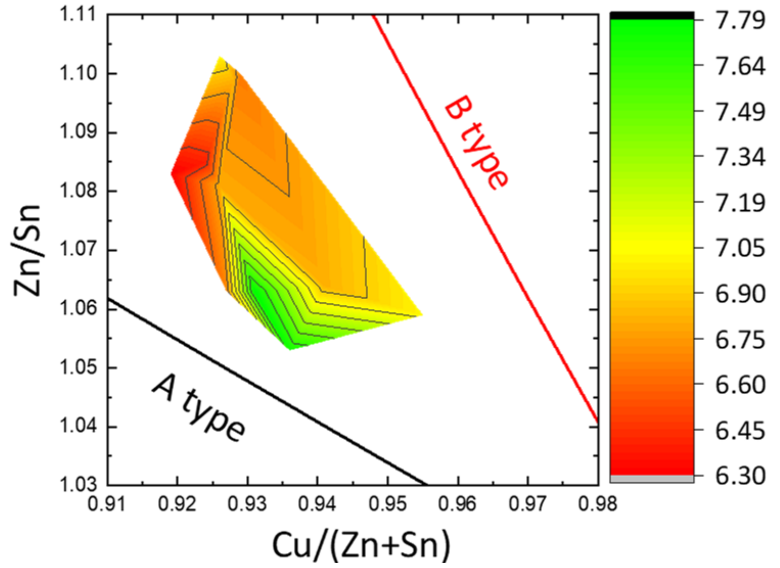

G. Gurieva et al, Sol. En. Mat. Sol. Cells 248 (2022) 112009

(i) Cu-Zn disorder in kesterite-type materials

(ii) off-stoichiometry in kesterite-type materials

(iii) off-stoichiometry in quaternary chalcogenides – „kesterite-derived“ materials

(iv) structural disorder in ternary nitrides

(v) Structural disorder hybrid halide perovskites?

Quaternary chalcogenide semiconductors … „kesterite-derived“ materials

main common structural feature of chalcogenide compound semiconductors: tetrahedral coordination

$A_2^{I}B^{II}C^{IV}X_4^{VI}$

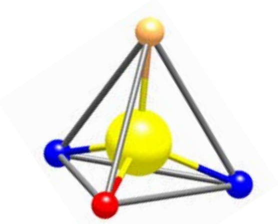

Stannite structure

(space group $I\bar{4}2m$)

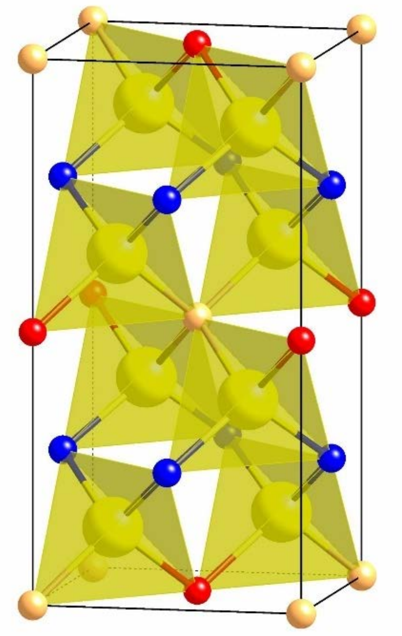

Kesterite structure

(space group $I\bar{4}$)

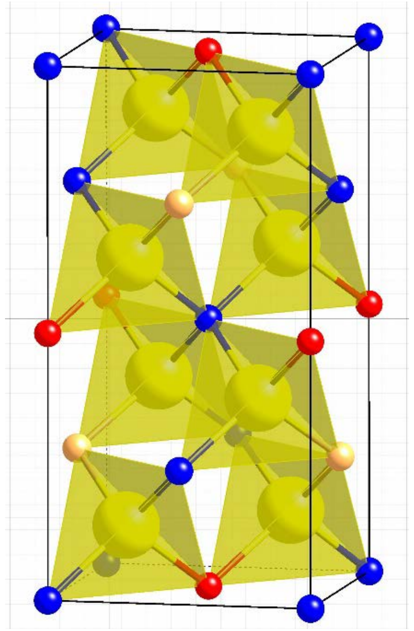

Wurtz-Stannite structure

(space group $Pnm2_1$)

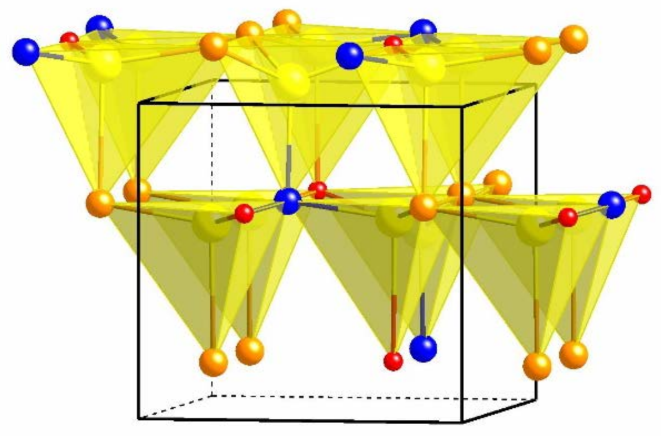

Wurtz-Kesterite structure

(space group Pn)

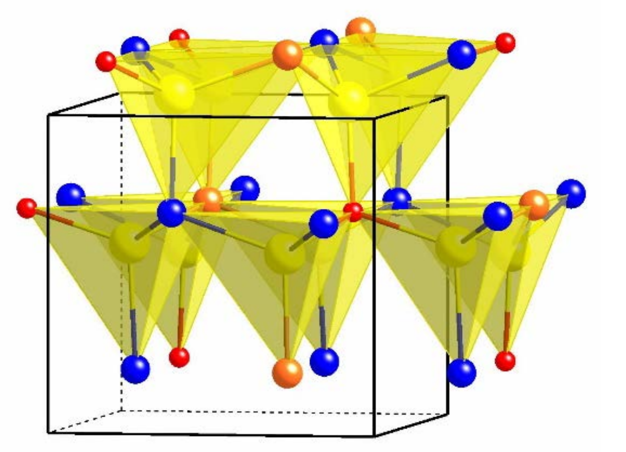

increase of distortion and tilting of the anion tetrahedra

symmetry decreases

Cu/B^{II} disorder – Kesterite vs. Stannite structure

Kesterite-type structure (s. g. $I\bar{4}$)

S. R. Hall et al., Can. Mineral. 16 (1978) 131

Cu – 2a & 2c

B^{II} – 2d

$(00l)$ lattice planes occupied by Cu and Zn

→ **Cu/Zn disorder**

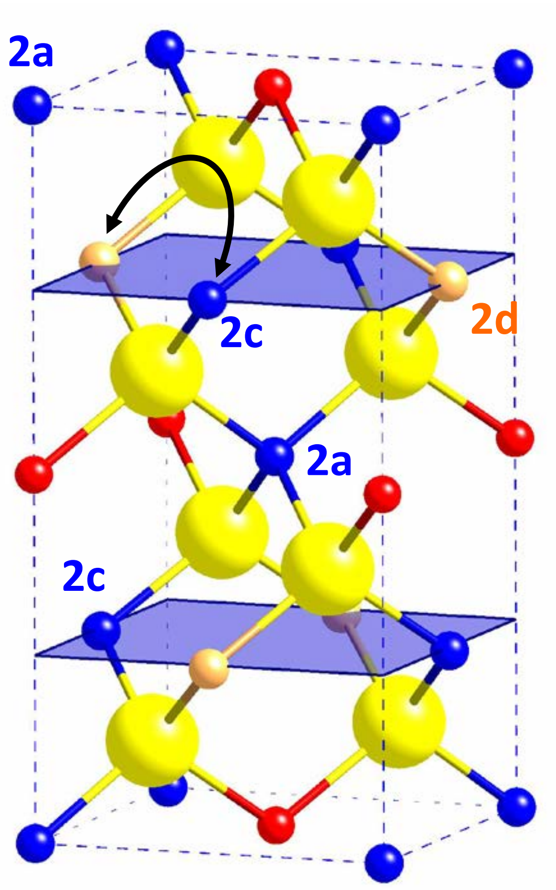

CZTS: Schorr et al., Europ. J. Mineral. 19 (2007) 65.
CZTSe: Schorr et al., Sol En Mat Sol Cells 95 (2011) 1482.
CZGeSe: Gurieva et al., J. Phys. Chem. Solids 99 (2016) 100.

Stannite-type structure (s. g. $I\bar{4}2m$)

S. R. Hall et al., Can. Mineral. 16 (1978) 131

Cu – 4d

B^{II} – 2a

$(00l)$ lattice planes occupied by Cu only

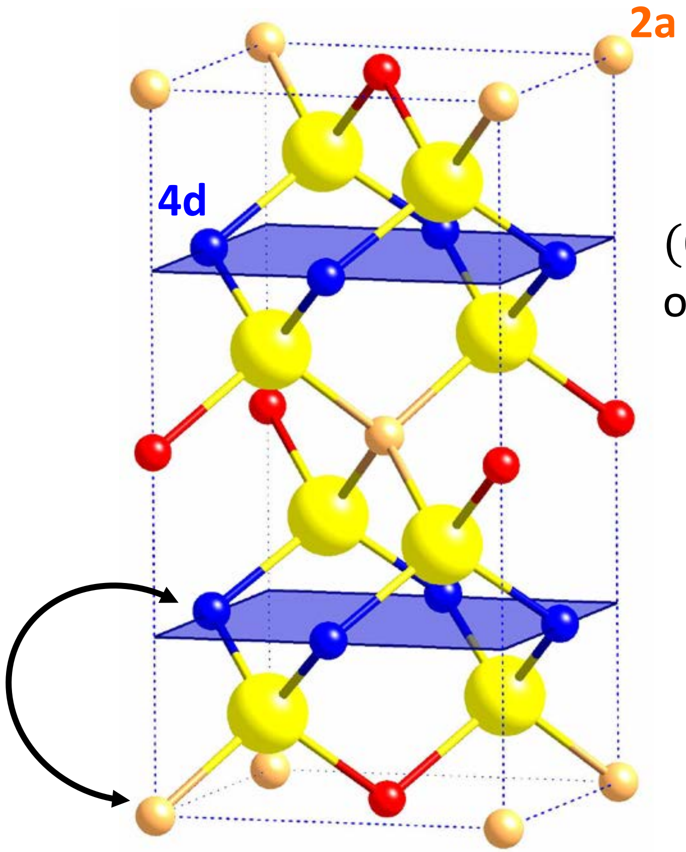

Cu/Mn disorder could occur on $(0k0)$ lattice planes

Cation and anion alloying: changes in the crystal structure

$Cu_2Mn(Ge,Sn)Se_4$

structure changes

$Cu_2MnGe(S,Se_4)$

w/o structure change

$Cu_2Mn(Ge,Sn)S_4$

structure changes

$Cu_2MnSn(S,Se_4)$

w/o structure change

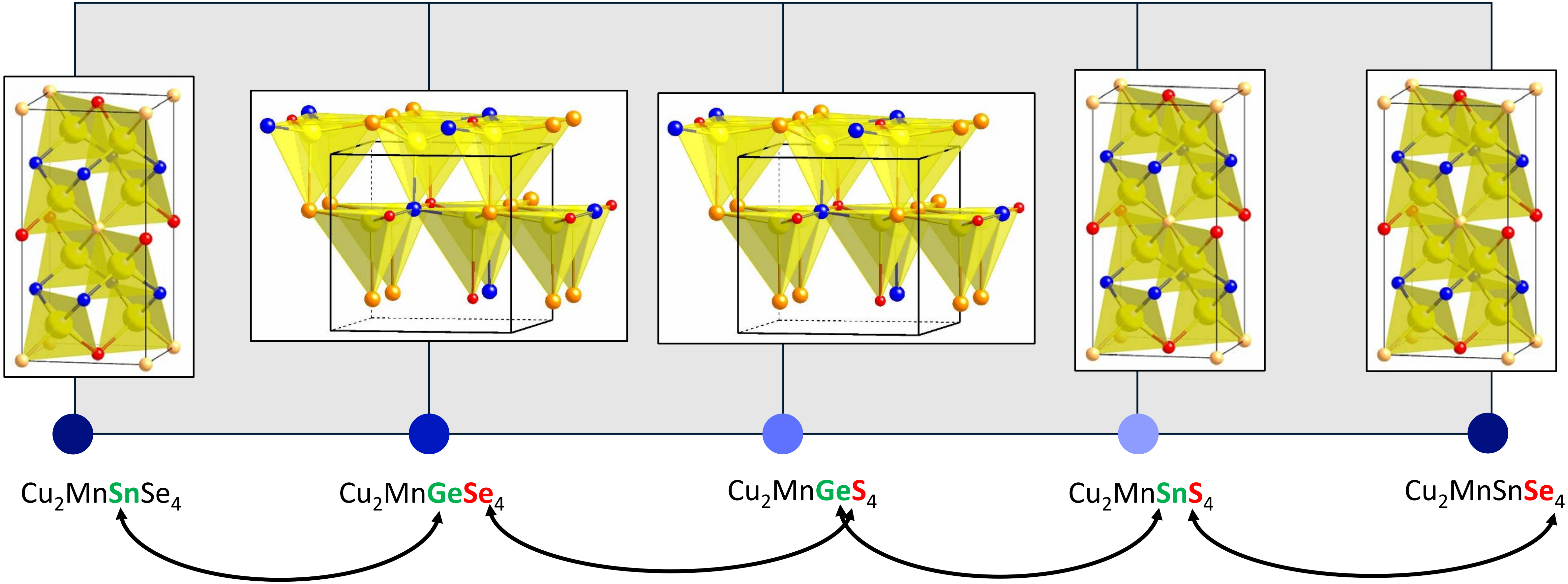

$Cu_2MnSnSe_4$

$Cu_2MnGeSe_4$

Cu_2MnGeS_4

Cu_2MnSnS_4

$Cu_2MnSnSe_4$

cation exchange

anion exchange

cation exchange

anion exchange

Cu_{Mn} & Mn_{Cu} in Stannite-type $Cu_2MnSnSe_4$ and $Cu_2MnSnSe_4$ …

Cation distribution on the 4d site (copper site) in off-stoichiometric Stannite-type $Cu_2MnSnSe_4$ …

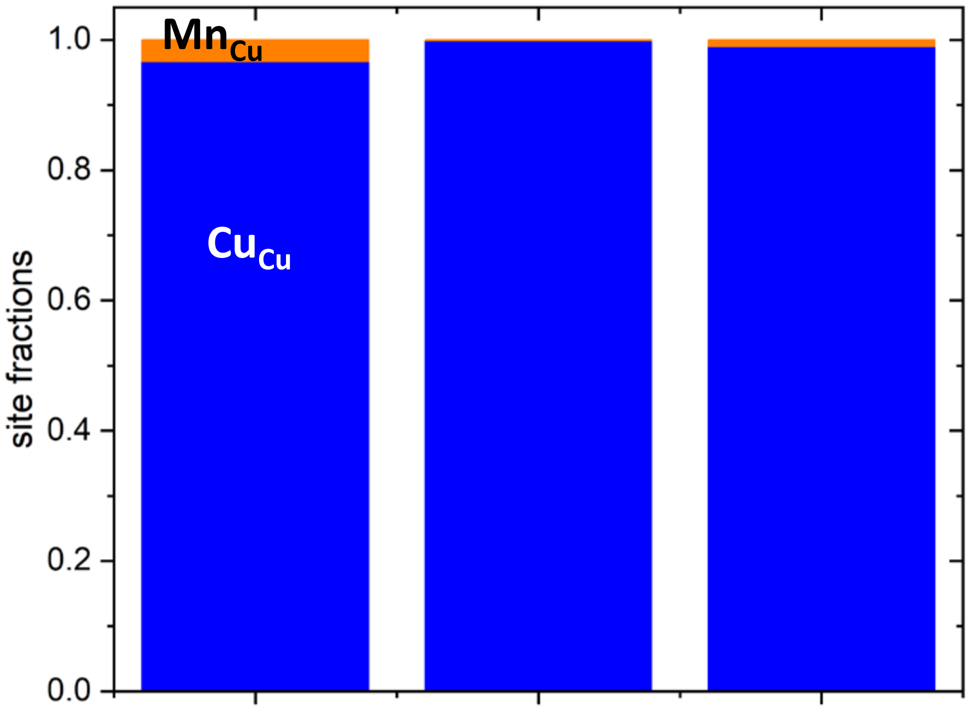

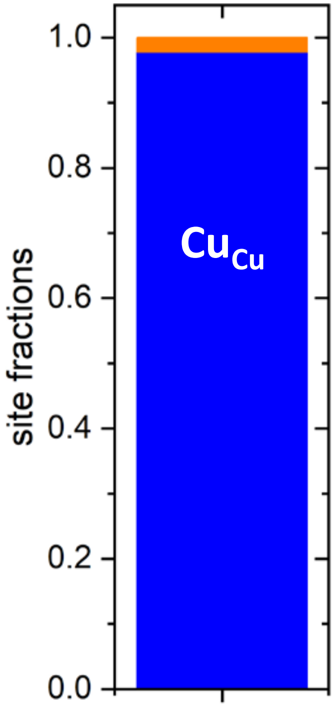

off-stoichiometric Kesterite-type Cu_2ZnSnS_4

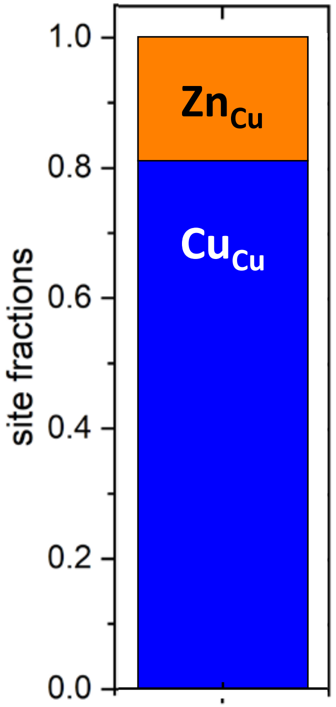

Cu/(Mn+Sn)	1.036	1.068	1.079	0.971	0.967
Mn/Sn	0.988	0.964	0.931	1.055	1.066

→ formation of Cu_{Mn} & Mn_{Cu} anti site defects, but with very low fractions (< 0.05)

→ Cu/Mn swapping

→ fractions of Cu_{Zn} & Zn_{Cu} >> 0.05 Cu/Zn disorder

Structural disorder: Cu_{Mn} and Mn_{Cu} anti-sites

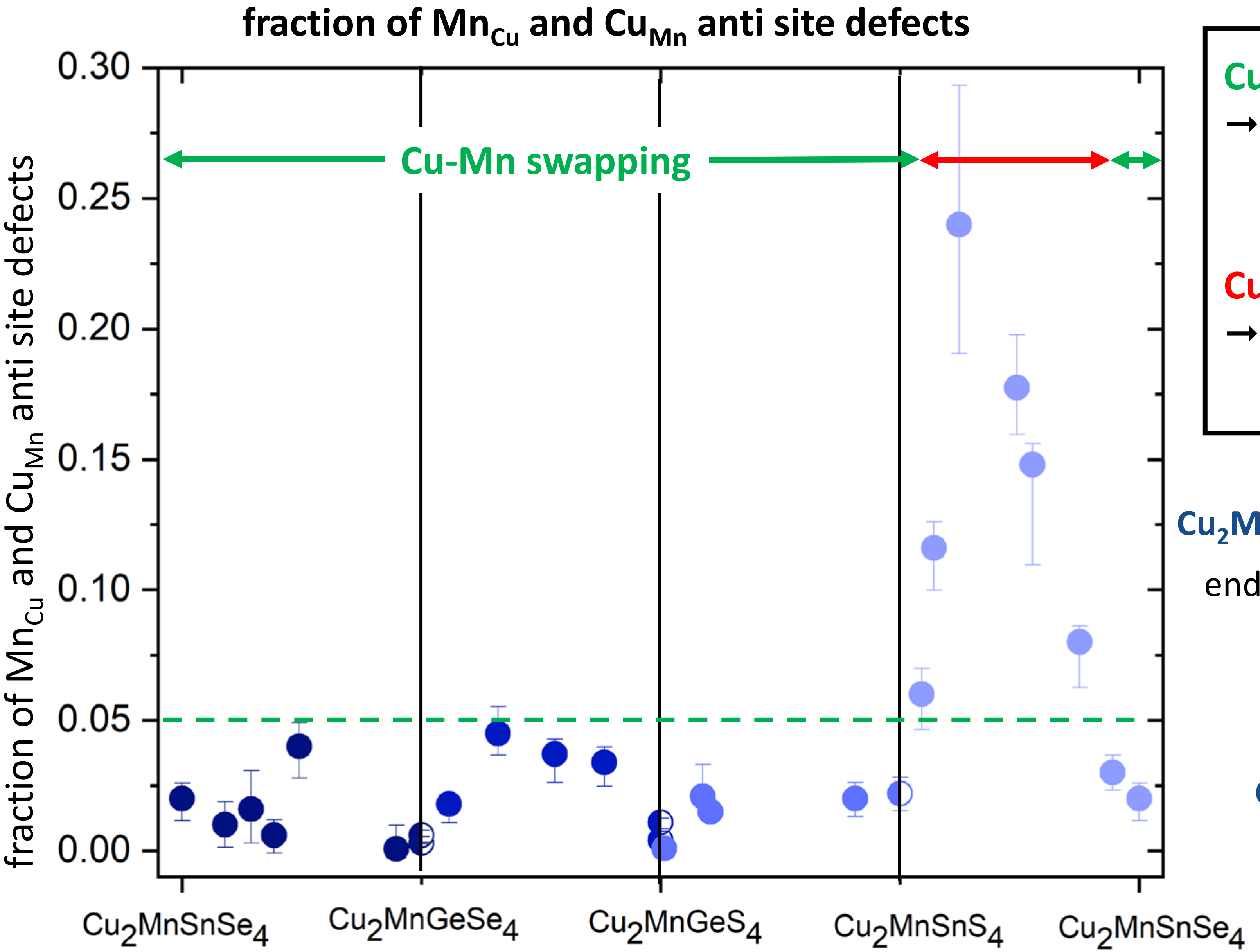

Cu-Mn swapping

→ formation of Cu_{Mn} and Mn_{Cu} anit site defect pairs with **fraction ≤ 0.05**

Cu/Mn disorder

→ formation of Cu_{Mn} and Mn_{Cu} anit site defect pairs with **fraction > 0.05**

$Cu_2Mn(Ge,Sn)Se_4$, $Cu_2MnGe(S,Se_4)$, $Cu_2Mn(Ge,Sn)S_4$

end members and mixed crystals

fraction of Cu_{Mn} & Mn_{Cu} < 0.05

→ **Cu-Mn swapping**

$Cu_2MnSn(S,Se_4)$ mixed crystals

fraction of Cu_{Mn} & Mn_{Cu} > 0.05

→ **Cu/Mn disorder**

Band gap energy – covers range of 0.9 eV … 2.1 eV

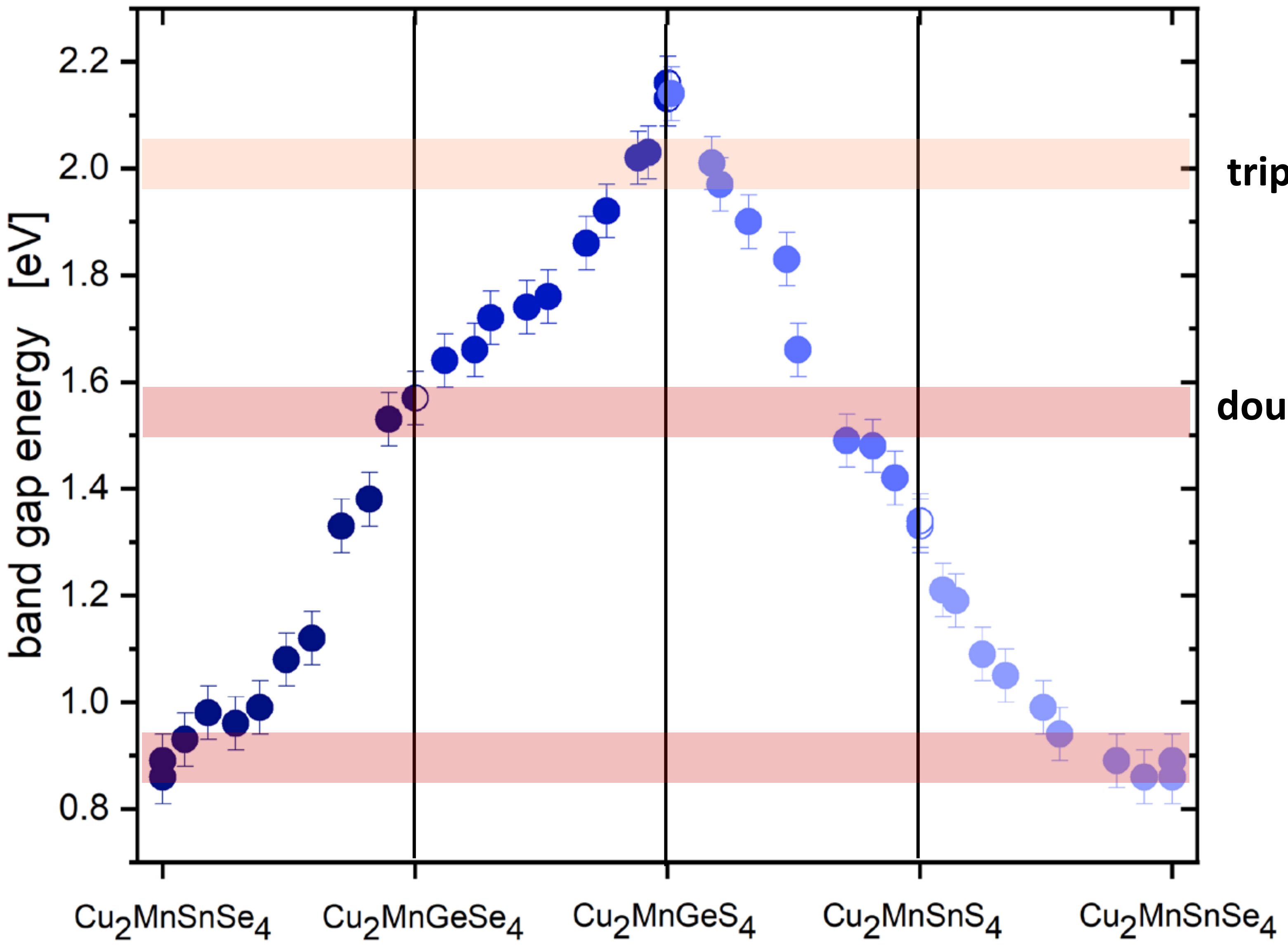

triple junction

double junction (tandem)

(i) Cu-Zn disorder in kesterite-type materials

(ii) off-stoichiometry in kesterite-type materials

(iii) off-stoichiometry in quaternary chalcogenides – „kesterite-derived“ materials

(iv) structural disorder in ternary nitrides

(v) Structural disorder hybrid halide perovskites?

Sustainable absorber materials for thin film solar cells

ternary nitrides (II-IV-N_2)

- earth-abundant alternatives to III-V compounds
- comparable band gap energies and lattice parameters

$ZnSiN_2$ / $ZnGeN_2$ / $ZnSnN_2$

- very efficient optical absorbers and emitters with a direct band gap
- device efficiency ($ZnSnN_2$, simulated) → 22%*

Band gap tuning mechanisms

- chemical alloying
- cation order/disorder

N. C. Coronel et al., PVSC & IEEE (2012) 003204.

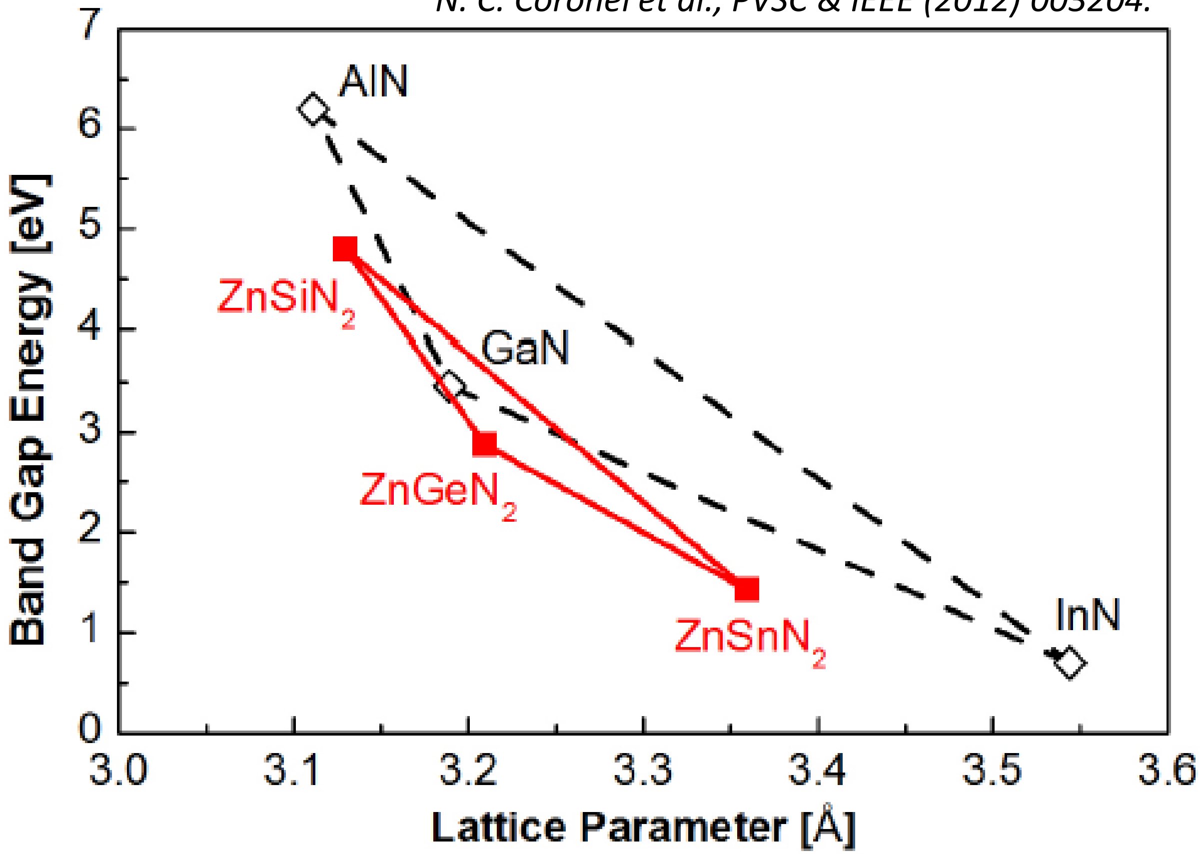

**Laidouci et al.,Sol. En. 211 (2020) 237.*

Symmetry relations in ternary nitrides (e. g. $ZnGeN_2$)

Wurtzite-type structure

$P6_3mc$

one cation site

2b $\left(\frac{1}{3},\frac{2}{3},0\right)$

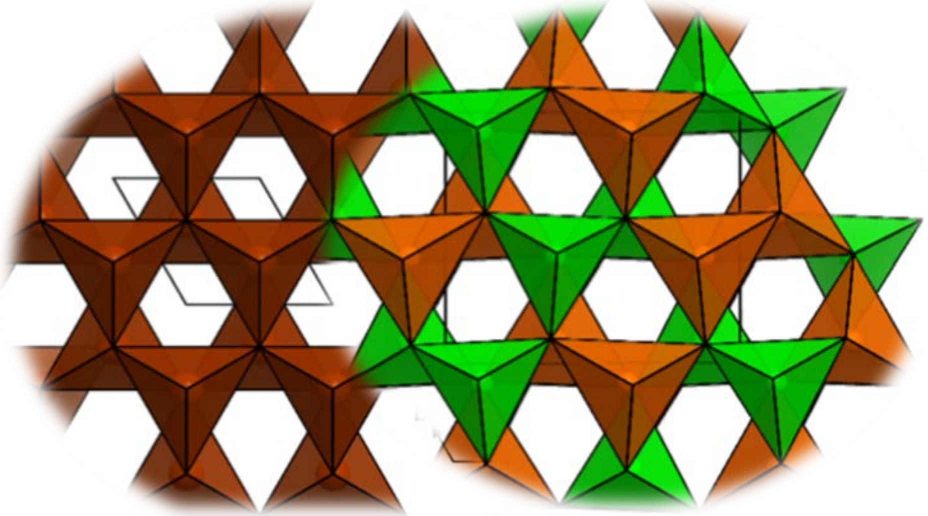

β-$NaFeO_2$-type structure

$Pna2_1$

two cation sites

4a (x_1, y_1, z_1)

4a (x_2, y_2, z_2)

Zn – Ge disorder

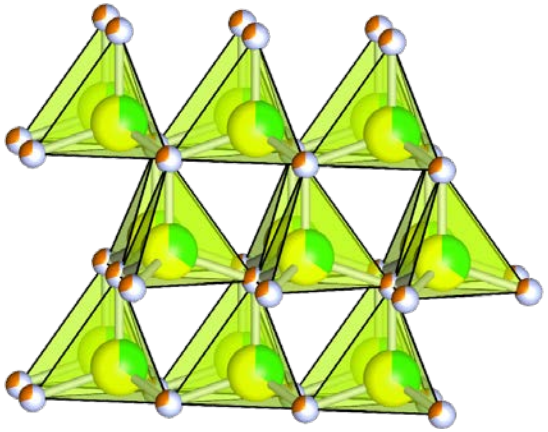

ordered distribution of Zn & Ge

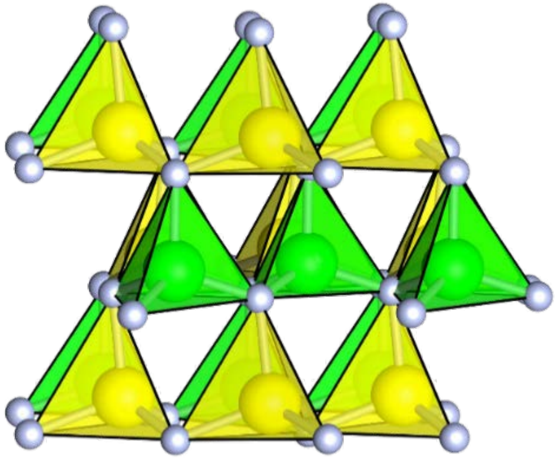

Our approach for a systematic study of structural disorder in $ZnGeN_2$

synthesis of powder samples

ammonolysis of oxide precursor (Zn_2GeO_4)
at reaction temperatures 750 – 910°C

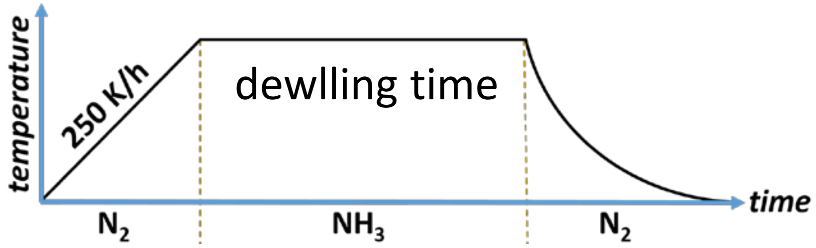

chemical analysis

- → XRF spectroscopy: Zn, Ge
- → hot-gas extraction: N, O

synthesized material always contain a certain amount of oxygen

→ **$Zn_{1+x}Ge_{1-x}(N_{1-x}O_x)_2$**

Breternitz et al., Phys. Stat. Solidi A 216 (2019) 1800885.
Wang et al., Chemical Science (2021) DOI: 10.1039/d1sc00328c

X-ray diffraction

$ZnGeN_2$

↓ |

Zn^{2+} and Ge^{4+} are isoelectronic
→ very similar atomic form factor *f*

↓

nitrogen is a light element
→ low X-ray scattering cross section

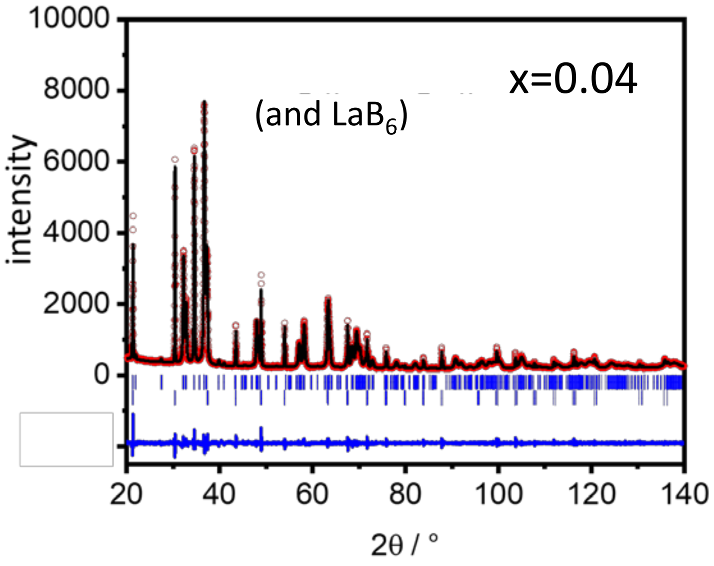

neutron diffraction

experiments performed at
E9 @ BERII (Berlin, Germany) and
D2B @ ILL (Grenoble, France)

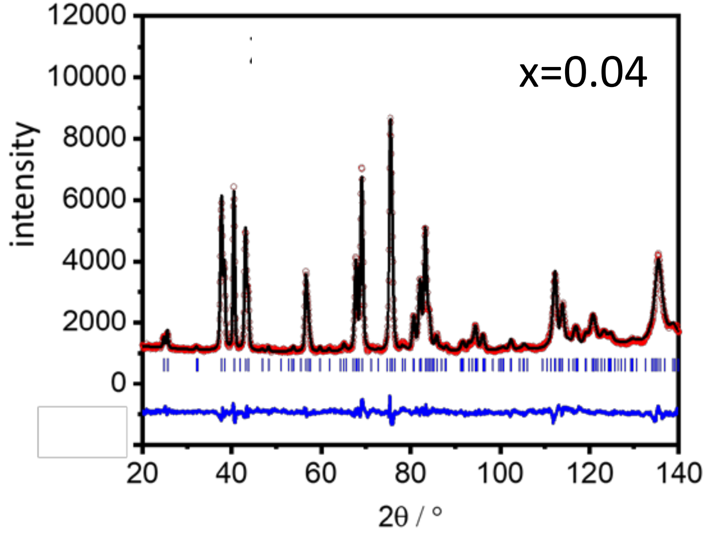

UV-ViS spectroscopy

→ determination of band gap energy E_g

Tunable oxygen content in $Zn_{1+x}Ge_{1-x}(N_{1-x}O_x)_2$ – tunable Zn/Ge ratio

chemical analysis

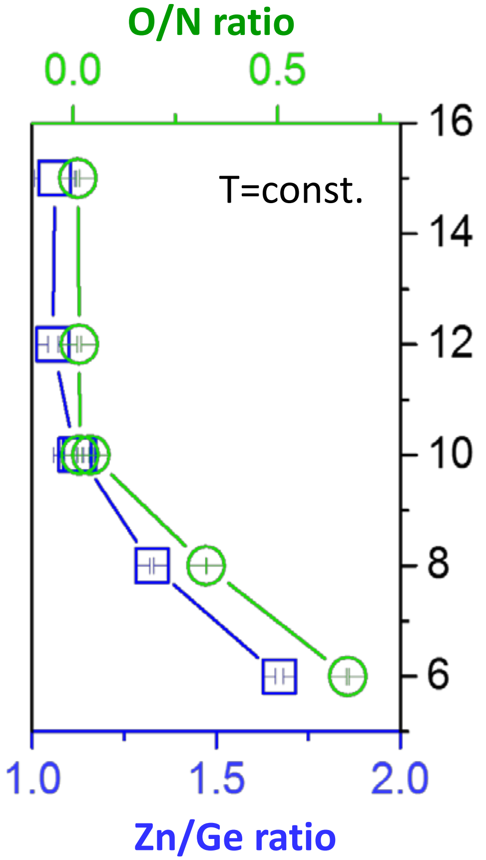

X-ray diffraction

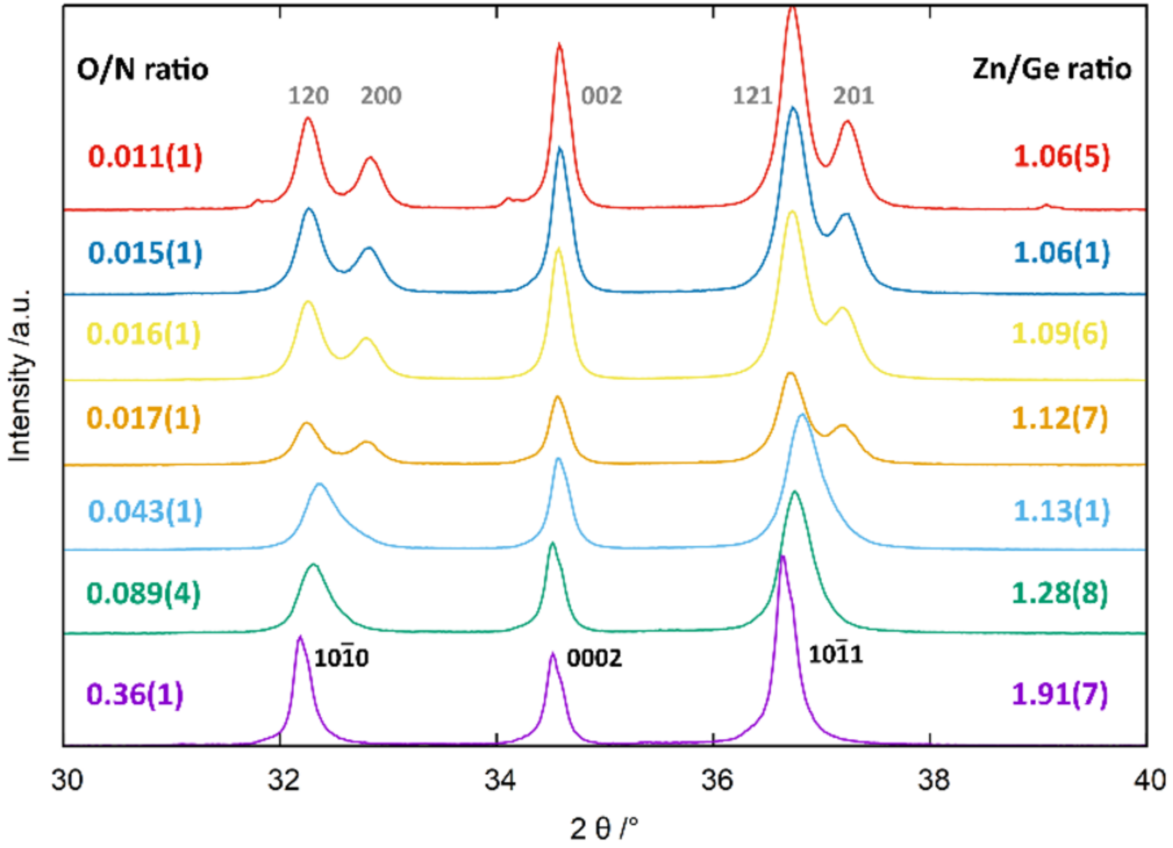

oxygen-poor:
β-$NaFeO_2$ type structure

oxygen-rich:
Wurtzite-type structure

Crystallization in the hexagonal Wurtzite structure or the orthorhombic β-$NaFeO_2$-type structure depends on oxygen content which can be tuned by the synthesis conditions (T, t)*

**Wang et al., Chemical Science (2021) DOI: 10.1039/d1sc00328c*

Cation distribution in $Zn_{1+x}Ge_{1-x}(N_{1-x}O_x)_2$

Cation distribution
determined by the analysis of SOF extracted by Rietveld refinement of **neutron diffraction data**

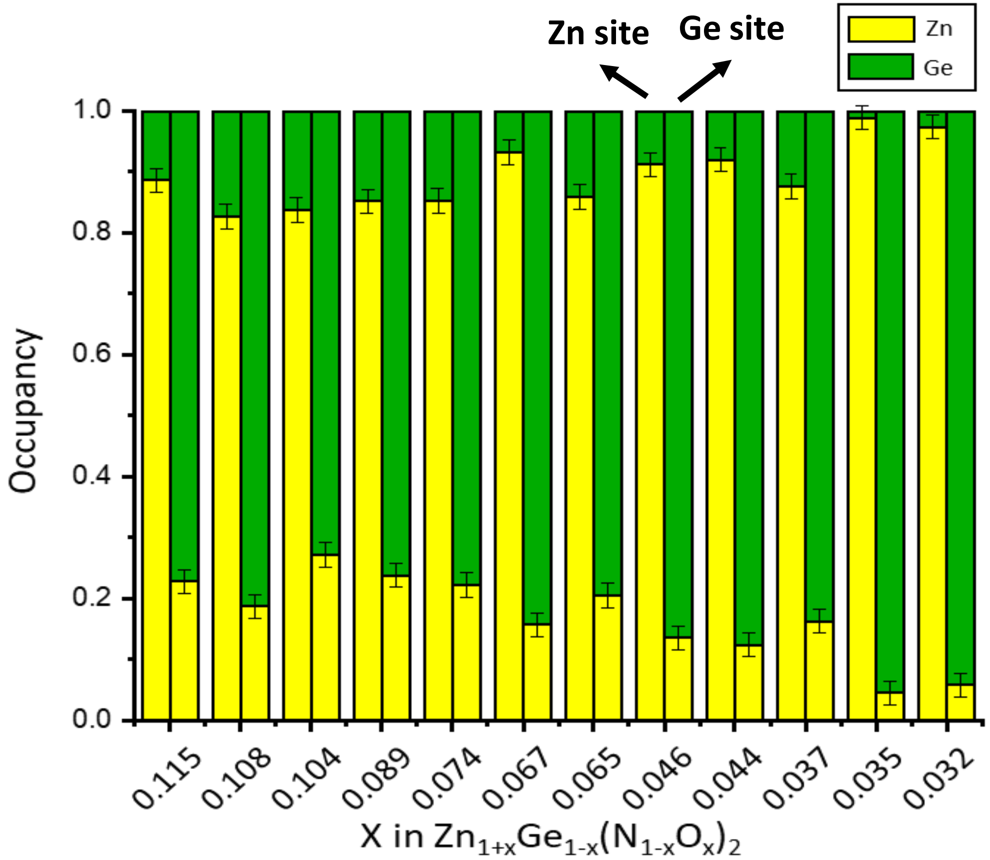

cation order

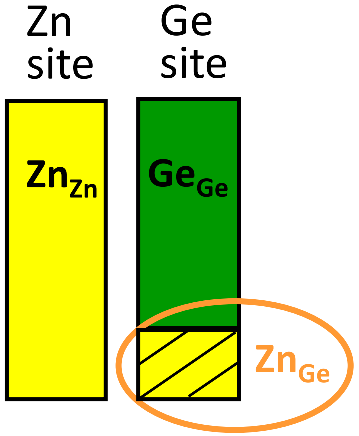

Zn_{Ge}: anti-site defect present due to Zn/Ge>1
→ depends on oxygen content

cation disorder

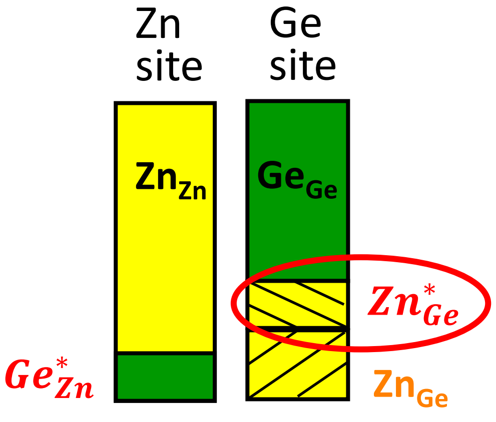

Zn_{Ge}: anti-site defect present due to Zn/Ge>1
→ depends on oxygen content

AND

Zn^{*}_{Ge} & Ge^{*}_{Zn}
anti-site defects
as **intrinsic disorder**
→ (in)dependent on oxygen content?

Wang et al., J. Mat. Chem. C 12 (2024) 1124-1131

Correlates intrinsic cation disorder Ge^{*}_{Zn} with oxygen content x?

general trend
increasing oxygen content ↳ increasing intrinsic cation disorder

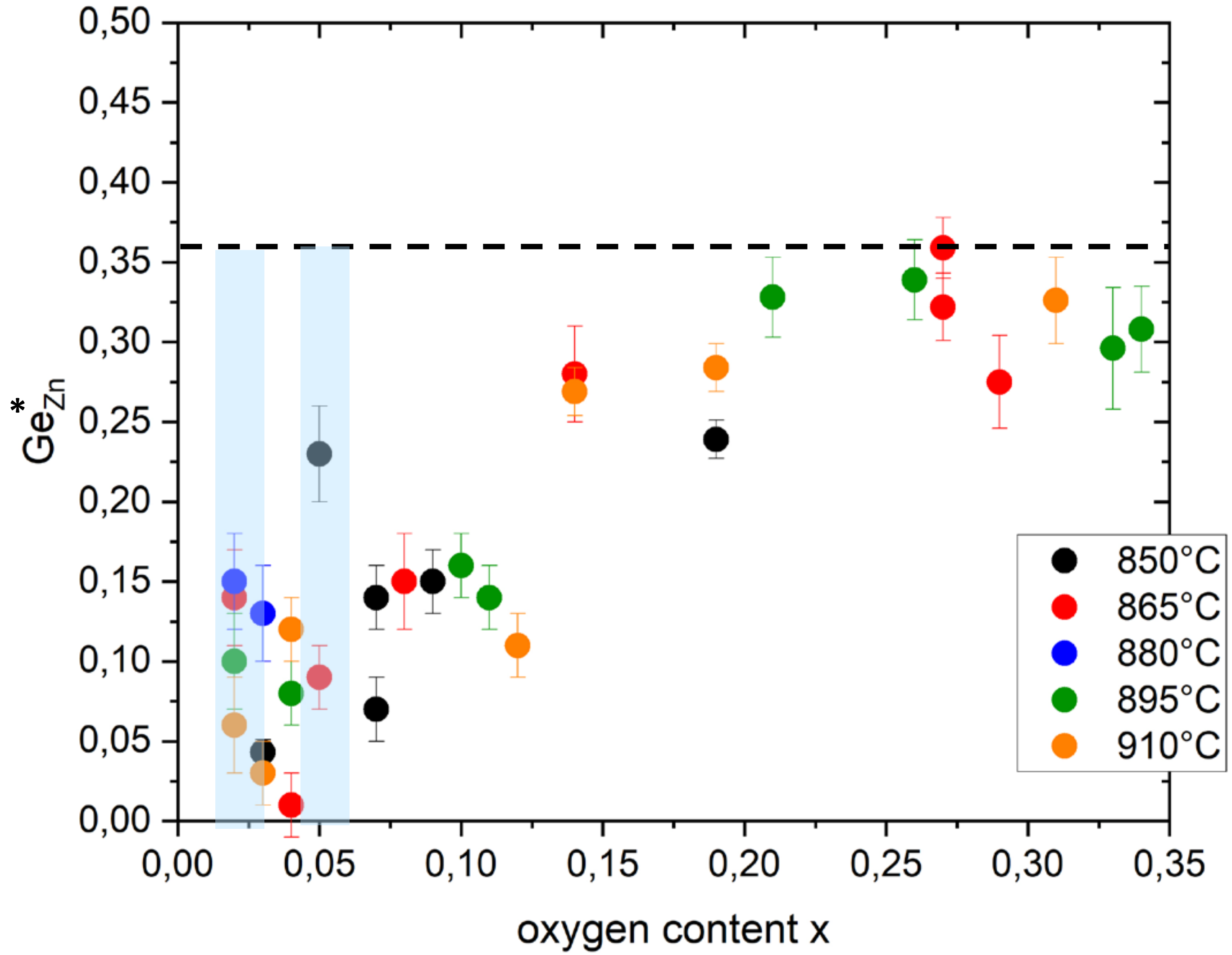

- **$Zn_{1+x}Ge_{1-x}(N_{1-x}O_{x})_2$ with same oxygen content show differerent intrinsic disorder Ge^{*}_{Zn}**

- **limit for intrinsic disorder Ge^{*}_{Zn}**

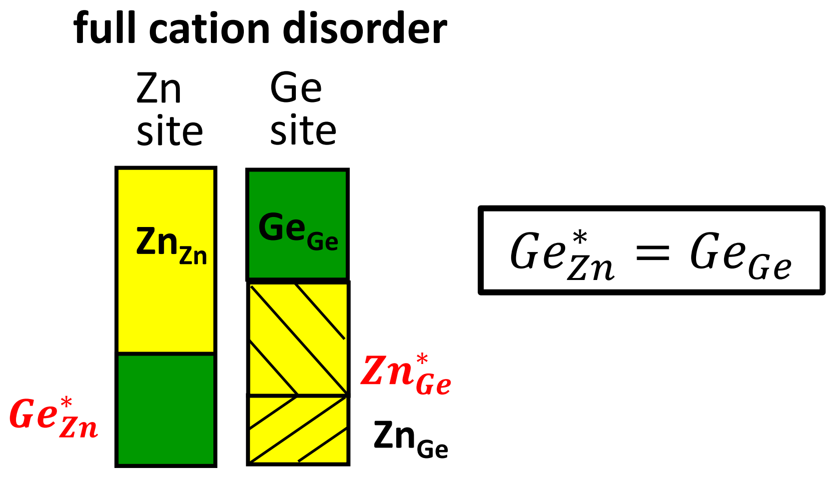

full cation disorder

Zn site
Ge site

Zn_{Zn}
Ge_{Ge}
Ge^{*}_{Zn}
Zn^{*}_{Ge}
Zn_{Ge}

$$\boxed{Ge^{*}_{Zn} = Ge_{Ge}}$$

Wang et al., J. Mat. Chem. C 12 (2024) 1124-1131

Quantification of cation disorder: order parameter

order parameter = 1

… $Ge^*_{Zn} = 0$

order parameter = 0

$Ge_{Ge} = Ge^*_{Zn}$ is fullfilled when half of the Ge occupies the Zn site

order parameter

$$1 - \frac{Ge^*_{Zn}}{Ge/2}$$

fully ordered

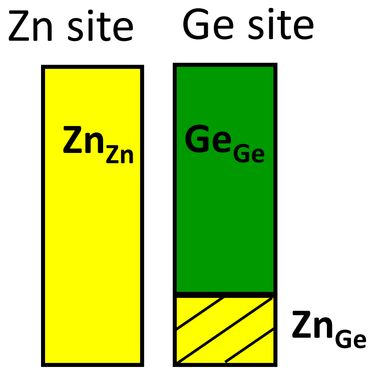

$$\boxed{Ge^*_{Zn} = 0}$$

fully disordered

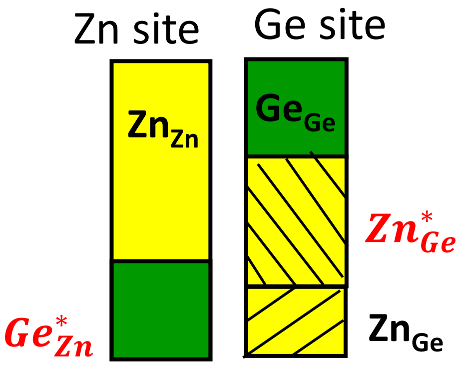

$$\boxed{Ge^*_{Zn} = Ge_{Ge}}$$

$Ge = Ge_{Ge} + Ge^*_{Zn}$

- Ge content in $Zn_{1+x}Ge_{1-x}(N_{1-x}O_x)_2$

→ depends on oxygen content
($Ge = 1 - x$)

- Ge^*_{Zn} in $Zn_{1+x}Ge_{1-x}(N_{1-x}O_x)_2$

→ independent on oxygen content

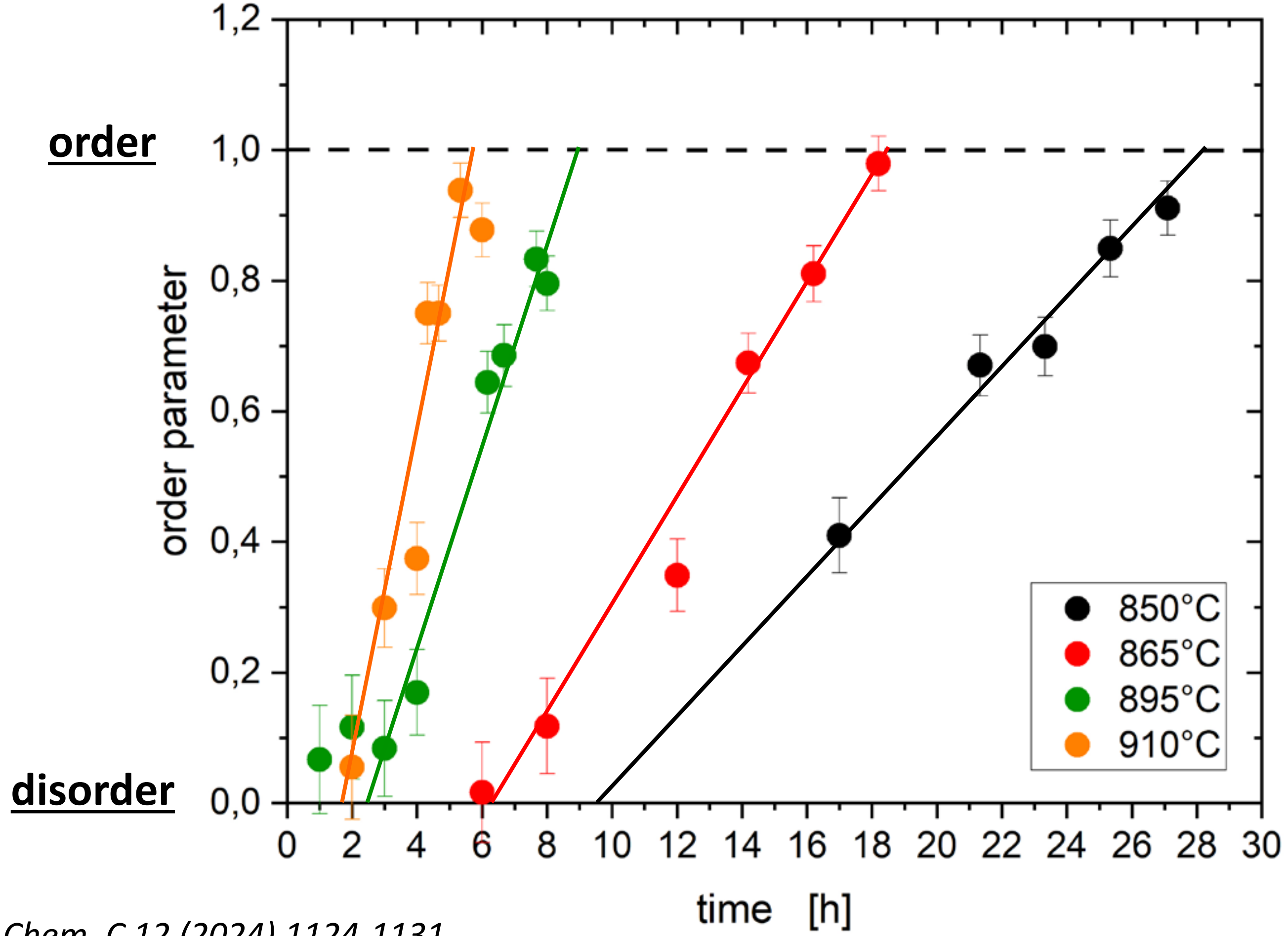

Wang et al., J. Mat. Chem. C 12 (2024) 1124-1131

Band gap energy E_g in $Zn_{1+x} Ge_{1-x} (N_{1-x}O_x)_2$

E_g vs. oxygen content

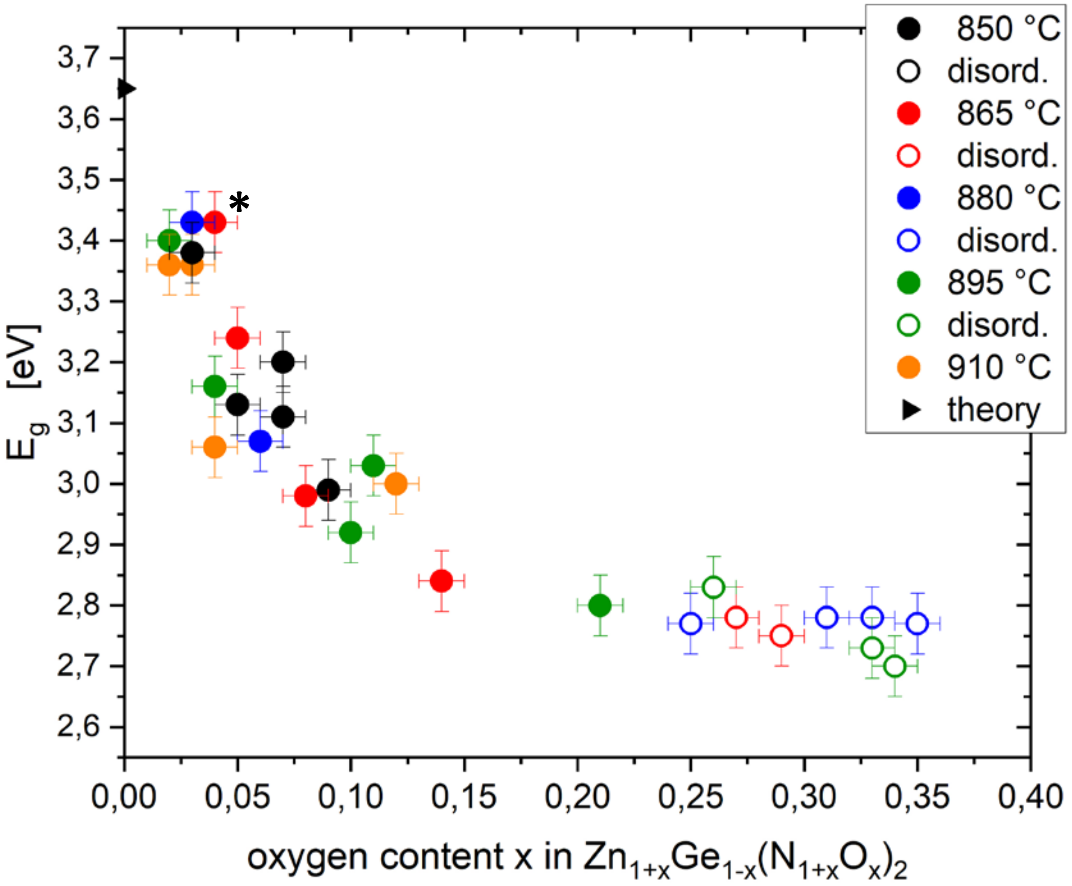

E_g vs. order parameter

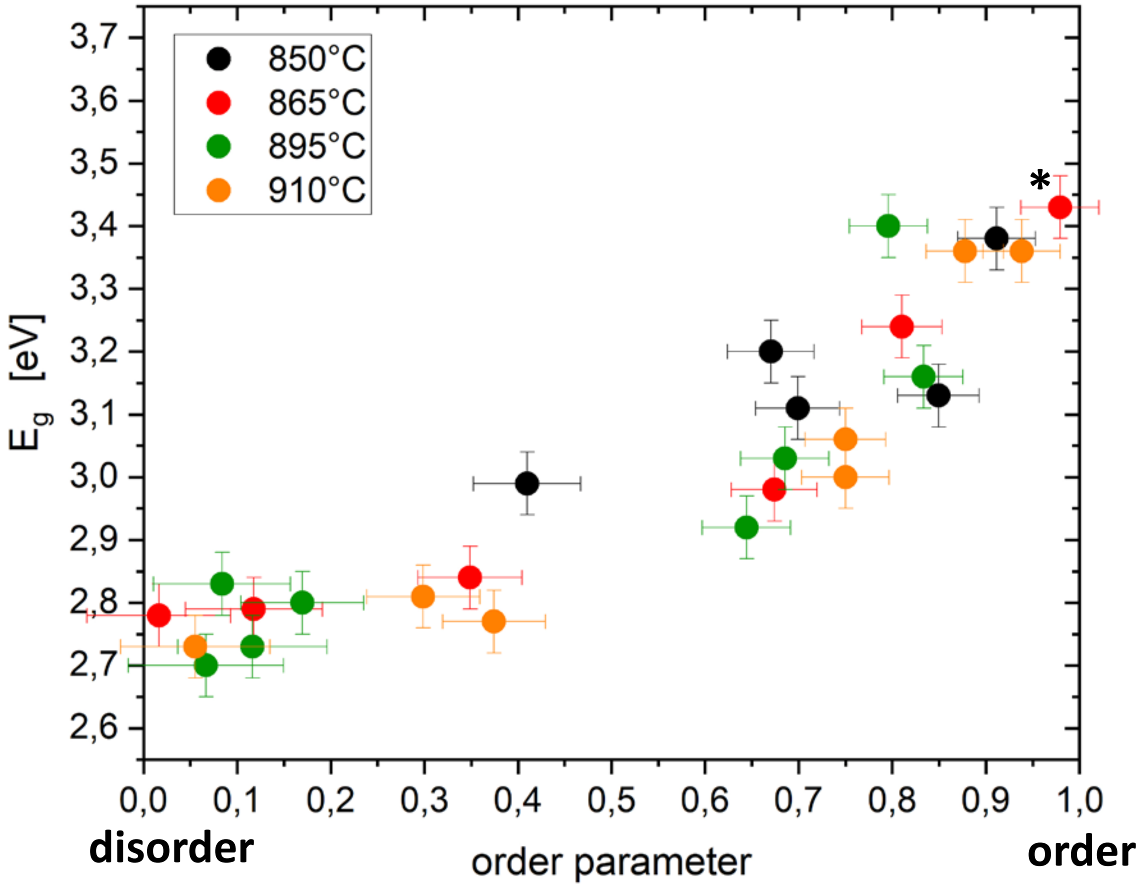

- **band gap energy E_g is influenced by oxygen content x AND intrinsic cation disorder BUT different**
- **$Zn_{1+x}Ge_{1-x}(N_{1-x}O_x)_2$ with almost no disorder (*) does not show the lowest oxygen content**
- **band gap energy E_g of full disordered $Zn_{1+x}Ge_{1-x}(N_{1-x}O_x)_2$ is constant**

Wang et al., J. Mat. Chem. C 12 (2024) 1124-1131

(i) Cu-Zn disorder in kesterite-type materials

(ii) off-stoichiometry in kesterite-type materials

(iii) off-stoichiometry in quaternary chalcogenides – „kesterite-derived“ materials

(iv) structural disorder in ternary nitrides

(v) Structural disorder in hybrid halide perovskites?

hybrid halide perovskites are defect tolerant …

Defect tolerance

defect tolerant semiconductors

- tendency of a semiconductor to keep its properties despite the presence of crystallographic defects
- high light conversion efficiency is maintained despite high concentration of point defects

Defect tolerance can be arised by

(i) Point defects can form **defect pairs** → electronically beinign complexes
example: chalcopyrites like Cu(In,Ga)Se_2

Zhang, Wei, Zunger, Phys. Rev. B 57 (1998) 9642

comprehensive study of point defects in chalcopyrites by neutron diffraction

Stephan, Schorr, Schock, APL 98 (2011) 091906
Stephan et al., APL 101 (2012) 101907
Stephan et al., J. Phys. Chem. Sol. 98 (2016) 309

(ii) point defects can be less harmfull if dominant traps within the band gap are energetically **close to valence or conduction band edges** (shallow)

(iii) point defects can be less harmfull if they have **low capture cross sections**

found for hybrid metal halide perovskites

↓

important factor behind the rapid increase of device efficiency

A.M. Genose et al., Nature Communication 13 (2022) 4715

Hybrid metal halide perovskites for PV applications

$MAPbI_3$ - MAPI

MA - methylammonium
$[CH_3NH_3]^+$

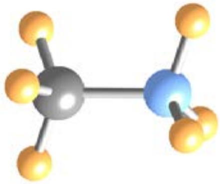

composition of the absorber layer of the record efficiency device

$(Cs,MA,FA)Pb(I,Br)_3$

FA … formamidinium
$[H_2NCH=NH_2]^+$

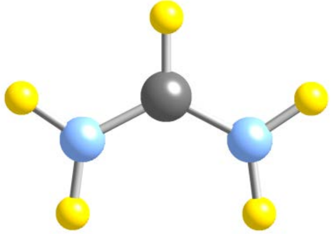

static structure (crystal structure) … perovskite structure

PbX_6 network → cornersharing octahedra (in non-cubic structures tilted and distorted)
→ electronic band structure of hybrid perovskites originates predominately from this network

organic cations in [12] coordination by the halide

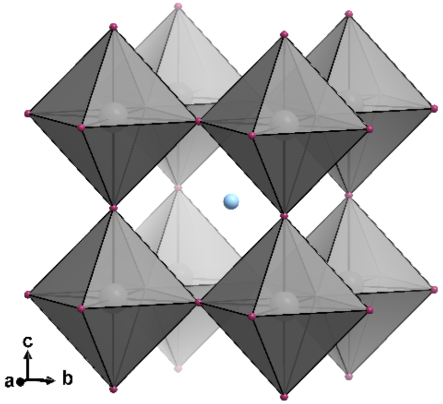

dynamic structure

organic cations → very flexible, large dipole moments
→ contributing to dynamic disorder and electrostatic screening

- orientational disorder of the molecules ⟶ **structural disorder**
- rotations of the molecule ⟶ quasielastic/inelastic neutron scattering

Perovskite structure – network of corner sharing PbX$_6$ octahedra

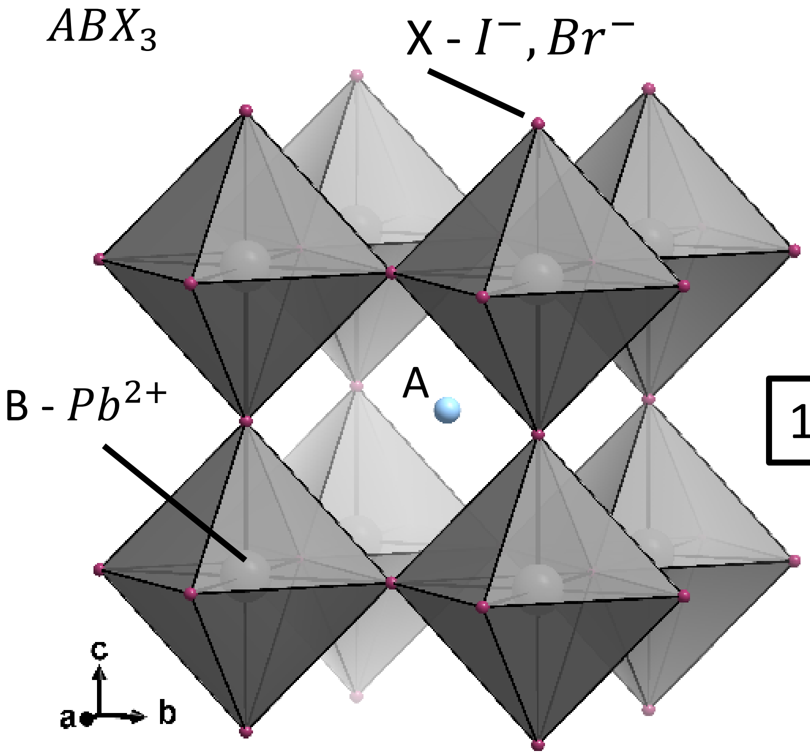

hybrid
halide perovskite

A - $[HC(NH_2)_2]^+$ (FA)
$[CH_3NH_3]^+$ (MA)

all-inorganic
halide perovskite

A … Cs^+

FA - Formamidinium
MA - Methylammonium

MAPbI$_3$

T > 330 K

161 K < T < 330 K

T < 161 K

cubic perovskite (α-phase)
(space group $Pm\overline{3}m$)

- complete orientational disorder of the molecule (e. g. MAPbBr$_3$)

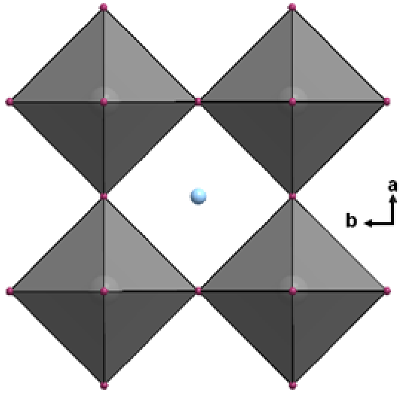

tetragonal perovskite (β-phase)
(space group $I4cm$)

- orientational disorder of the molecule (e. g. 8 orientations in MAPI$_3$)
- tilting of the PbX_6 octahedra (distortet)

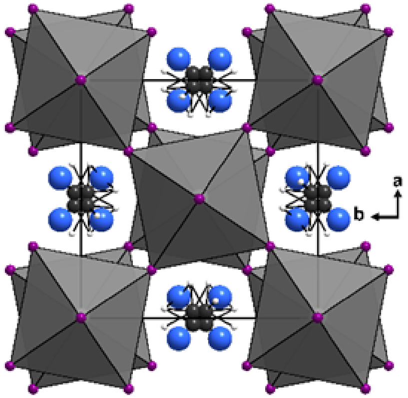

orthorhombic perovskite (γ-phase)
(space group $Pnma$)

- orientational disorder of the molecule (e. g. 2 orientations in MAPbCl$_3$)
- tilting and kinking of the PbX_6 octahedra (distortet)

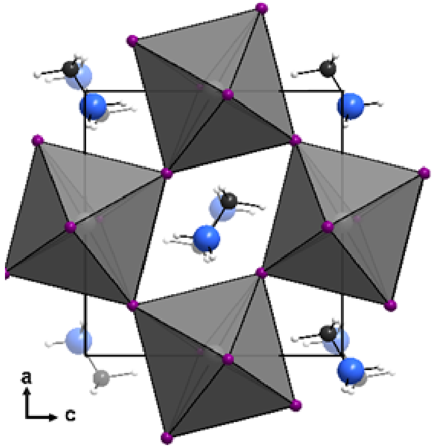

P. S. Whitfield et al., Sci. Rep. 6 (2016) 35685

Orientational disorder of the MA$^+$ molecule in MAPbI$_3$

synX-ray powder diffraction

@KMC-2 (BESSYII)

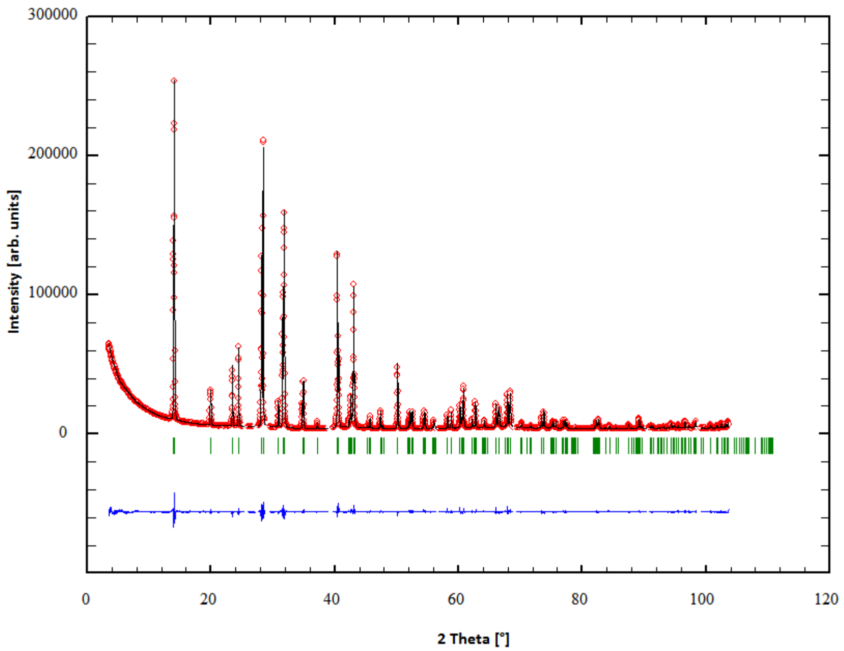

neutron powder diffraction

@E9 (BERII)

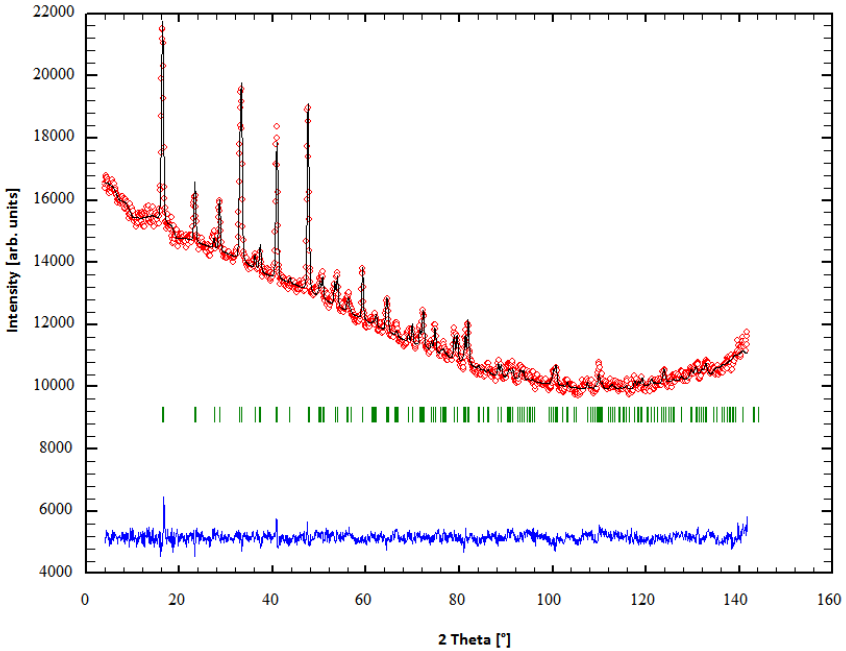

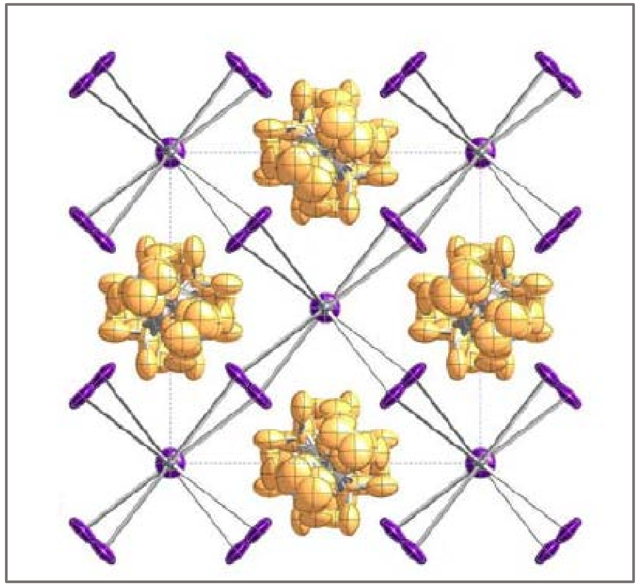

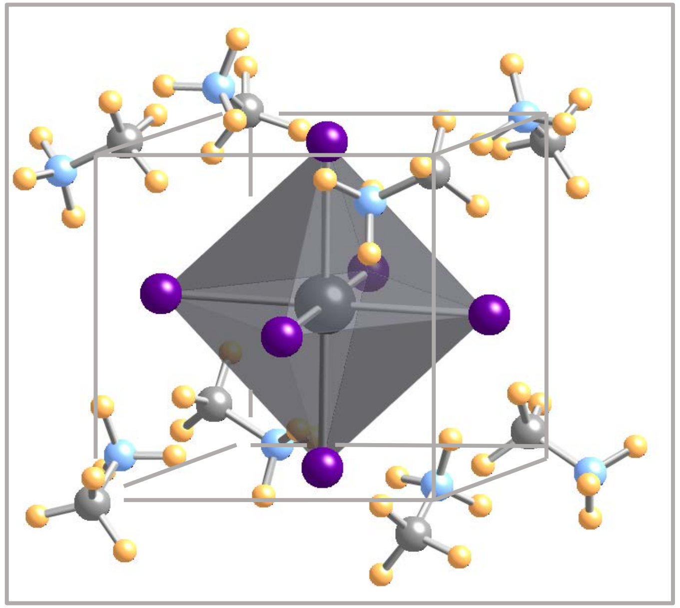

- Perovskite structure: space group $I4cm$ → non-centrosymmetric
- PbI$_6$ octaedra tilting occurs along [001]
- MA$^+$ molecules are aligned in <221> → 8 possible orientations
  → **8-fold disorder of MA$^+$ molecule**

A. Franz, D.M. Többens, S. Schorr, Cryst.Res.Technol. 51 (2016) 534

Fundamental reasoning of ferroelectricity in $MAPbI_3$

- crystal class (point group) which contains an inversion center as one of its symmetry elements is **centrosymmetric**
- **crystals with an inversion center cannot display certain properties, such as piezoelectricity**
- ferroelectric materials are also piezoelectric

crystal system	centrosymmetric	non-centrosymmetric
triclinic	$\bar{1}$	1
monoclinic	$2/m$	$2, m$
orthorhombic	mmm	$222, mm2$
tetragonal	$4/m, 4/mmm$	$4, \bar{4}, 422, 4mm, \bar{4}m2$
trigonal	$\bar{3}, \bar{3}m$	$3, 32, 3m$
hexagonal	$6/m, 6/mmm$	$6, \bar{6}, 622, 6mm, \bar{6}m2$
cubic	$m3, m\bar{3}m$	$23, \bar{4}3m, 432$

In literature so far:

crystal structure of MAPI → space group $I\frac{4}{m}cm$

→ centrosymmetric!

If this is true, MAPI cannot be ferroelectric!

$MAPbI_3$ is non-centrosymmetric at RT

our studies

- combined synchrotron X-ray (BESSYII) and neutron (BER) diffraction
- single crystal XRD at Diamond Light Source (GB) applying anomalous diffraction at the Pb edge

showed → MAPI adopts the space group $I4cm$

J. Breternitz et al., Angew. Chem. Int. Ed. 59 (2020) 424.

rotational dynamics of $(CH_3NH_3)^+$ (MA) ions in $MAPbI_3$

4-fold rotations of the molecule

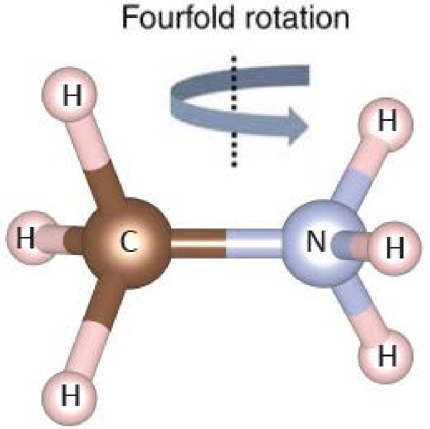

3-fold rotations of the molecule

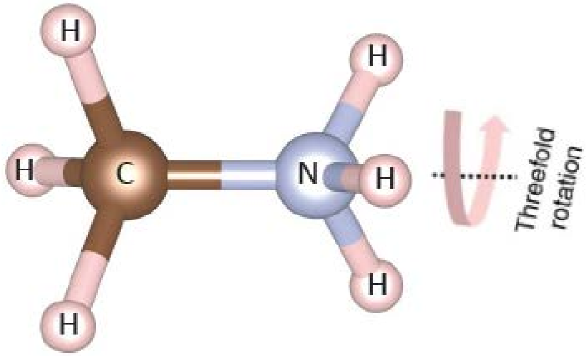

*Chen et al., Phys.Chem.Chem.Phys., **17** (2015) 31278*

quasi-elastic and inelastic neutron scattering (QENS, INS) @Institute Laue-Langevin (ILL), Grenoble, T=190 K – 70 K

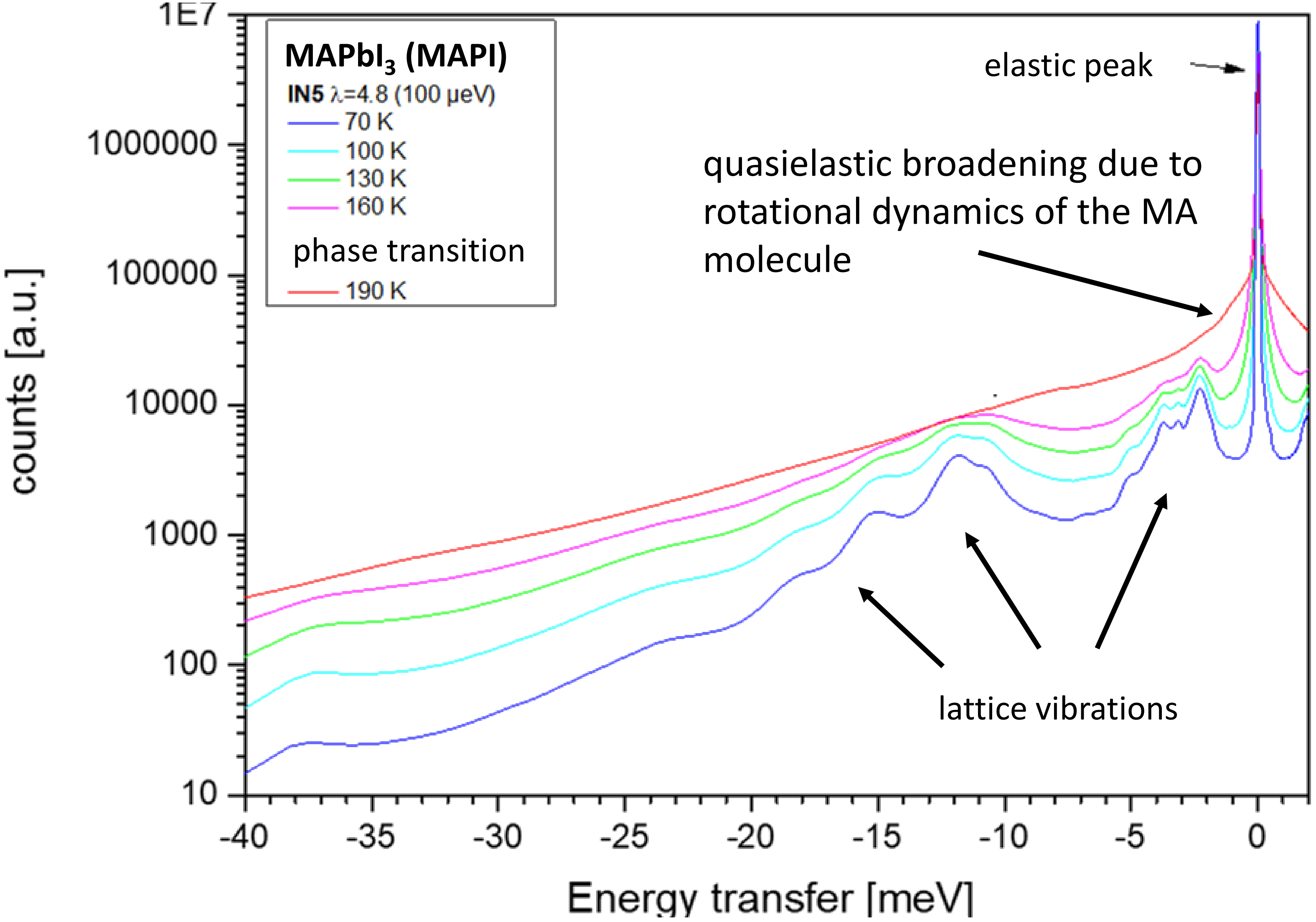

G. Schuck, D. M. Többens, …, and S. Schorr, J. Phys. Chem. C 122 (2018) 5227

Influence of chlorine on the hydrogen-halide bonding in halide perovskites

FTIR investigations indicate → **in the orthorhombic phase** (T < 161 K) **the iodide is more strongly influenced by hydrogen bonding than the chloride**

QENS data of $MAPbI_3$, $MAPbCl_3$ and $MAPb(I,Cl)_3$ T=70K

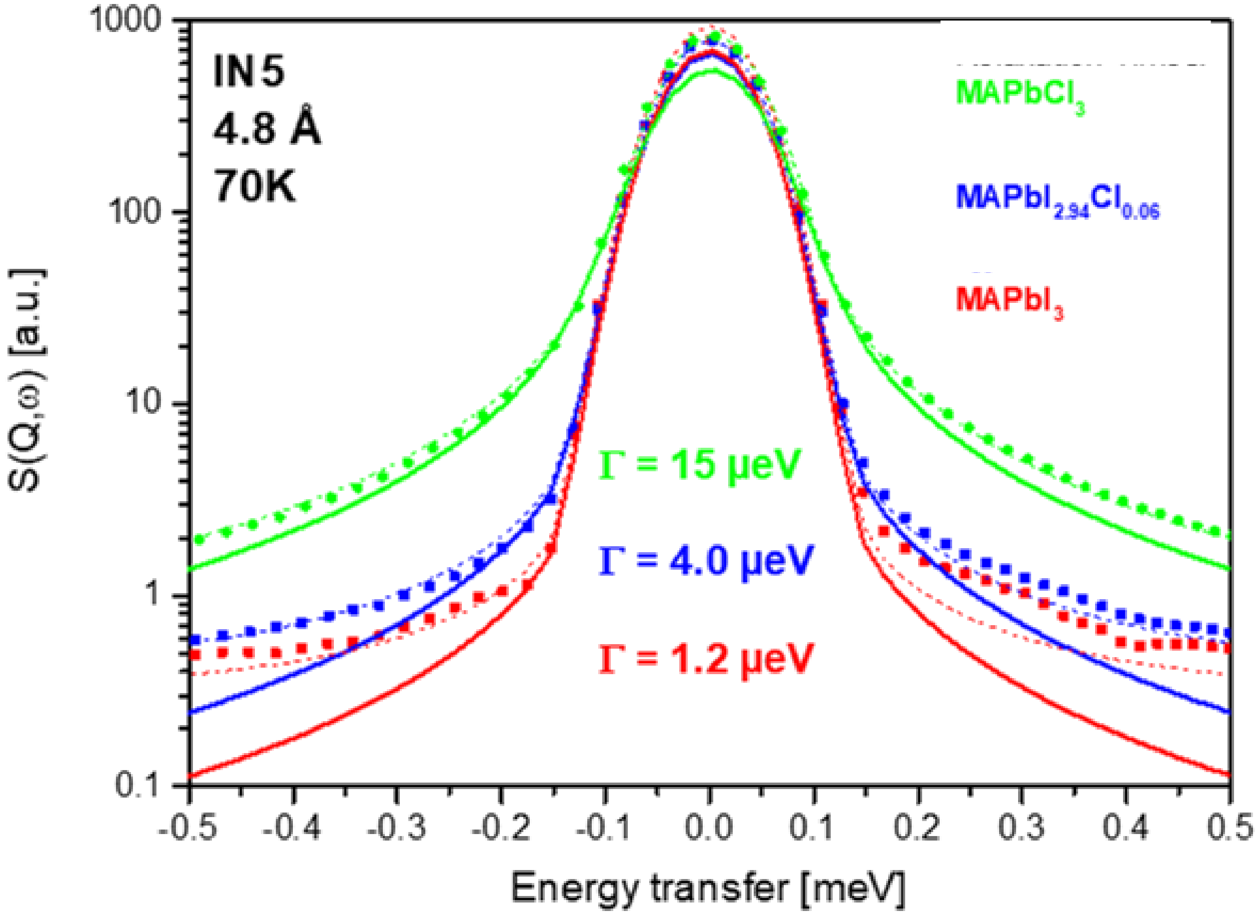

G. Schuck, D. M. Többens, M. Koch-Müller, I. Efthimiopoulos, and S. Schorr, J. Phys. Chem. C 122 (2018) 5227

MA molecule in cuboctahedral coordination by the halide

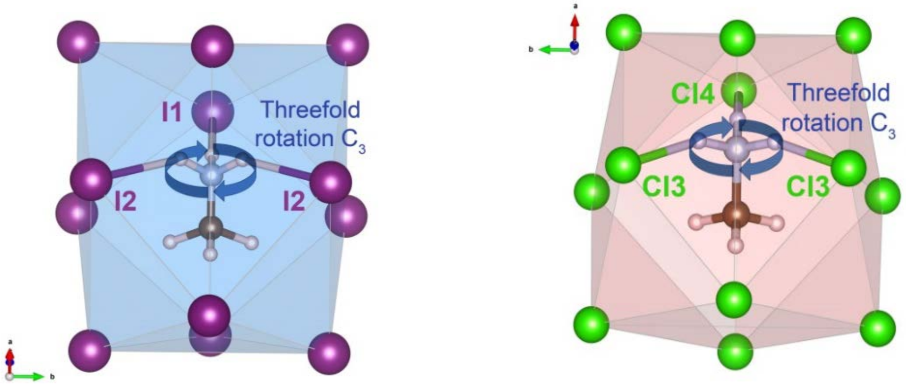

characteristic relaxation time τ of the C_3 jump rotation

$$\Gamma_{C3}[meV] = \frac{3\hbar}{\tau_{C3}[ps]}$$

1635 ps > 485 ps > 135 ps

Chlorine substitution in MAPI (orthorhombic phase)
→ leads to a weakening of the hydrogen bonds

G. Schuck et al., J. Phys. Chem. C 123 (2019) 11436

Activation energies: $MAPI_3$, $MAPbI_{2.94}Cl_{0.06}$ and $MAPbCl_3$

Temperature dependent behaviour of Γ_{C3}

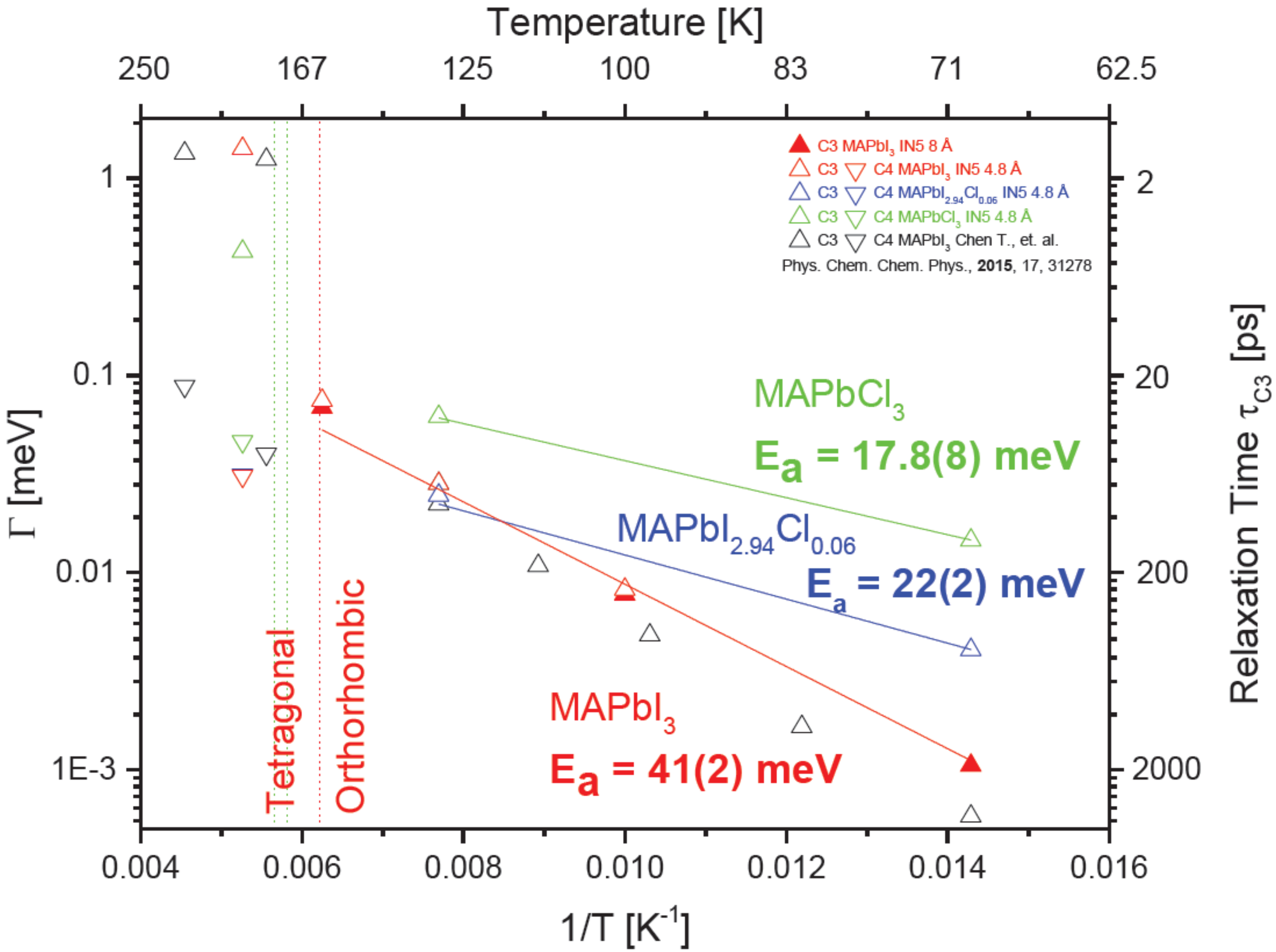

Activation energy E_a

$$\ln(\tau) = \frac{E_a}{k_B T} - \ln(A)$$

k_B: Boltzmann constant
A: pre-exponential factor

- E_a for to **$MAPbI_3$** in the range of literature data (Chen et. al. 2015)
- significant decrease of E_a in **$MAPbI_{2.94}Cl_{0.06}$** and **$MAPbCl_3$** compared to **$MAPbI_3$**

E_a also indicates that chlorine substitution leads to a weakening of the hydrogen bridge bonds in the orthorhombic phase

G. Schuck et al., J. Phys. Chem. C 123 (2019) 11436

Conclusions

- **intrinsic point defects determine electronic properties of semiconductors**
  - → their structural origin, defect type and concentration in correlation on chemical composition is crucial for **defect engineering** to improve the power conversion efficiency (PCE)

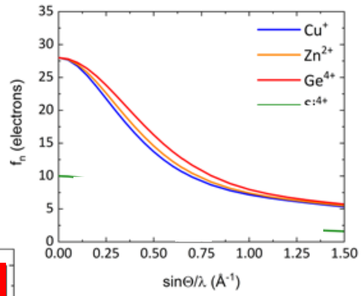

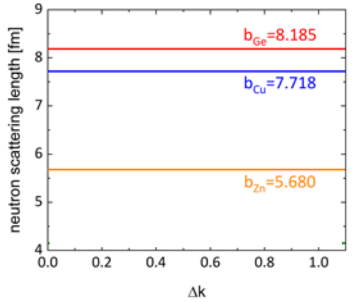

- **structural disorder can be derived by careful analysis of diffraction data**

- **structural disorder in kesterite-type solar absorbers**
  - → Cu_{Zn} & Zn_{Cu} anti-sites causing **Cu/Zn disorder**
  - → vacancies, anti-sites and interstitials caused by off-stoichiometry … off-stoichiometrytype model
  - → band gap energy changes with the off-stoichiometry type

Cu – Zn disorder

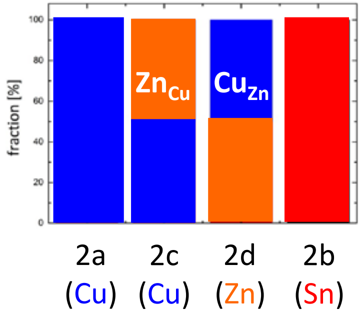

- **structural disorder in „kesterite-derived“ materials**
  - → Stannite-type and Wurtz-Stannite type $Cu_2Mn(Ge,Sn)(S,Se)_4$ compounds show **Cu-Mn swapping** (Cu_{Mn} & Mn_{Cu} < 0.05)

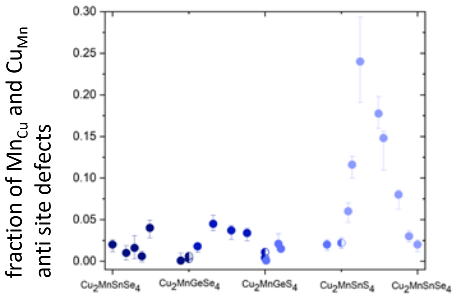

- **ternary nitrides ($ZnGeN_2$)**
  - → earth-abundant alternatives to III-V semiconductors
  - → Zn-Ge disorder correlates with the band gap energy

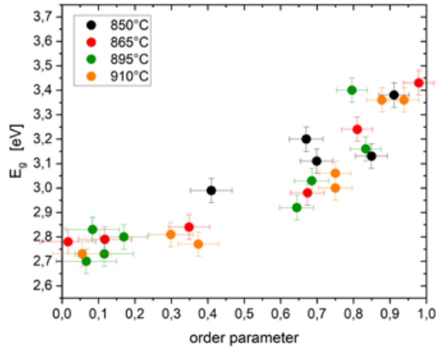

- **hybrid metal halide perovskites** are considered as defect tolerant structural disorder → orientational disorder of the molecule

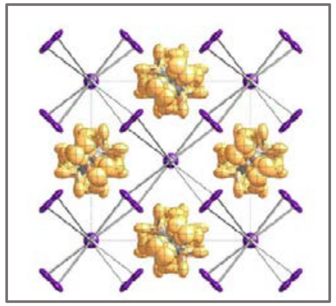

Acknowledgments

my colleagues from the Department Structure and Dynamics of Energy Materials at HZB

Dr. Galina Gurieva (quaternary chalcogenides)

Dr. Daniel Többens (KMC2-@BESSY II)

Dr. Joachim Breternitz (hybrid halide perovskites, ternary nitrides)

Dr. Kai Neldner (CZTS)
Dr. Elisa Valle-Rios (CZTSe)
Dr. Rene Gunder (CZGeSe)
Dr. Frederike Lehmann (MAPI)
Zhenyu Wang ($ZnGeN_2$)
} former PhD students

instrument scientists (neutron diffraction) at **neutron sources** all over the world
- former BERII at HZB, Germany
- Institute Laue-Langevin (ILL), Grenoble, France
- Paul-Scherrer-Institute (PSI), Villigen, Switzerland
- SNS, Oak Ridge National Lab, US
- ANSTO, Lucas Heights (near Sydney), Australia

instrument scientists (synX-ray diffraction) at **synchrotron radiation sources**
- ESRF, Grenoble, France
- Diamond Light Source, UK

KESTCELLS (2012-2015)

STARCELL (2017-2019)

INFINITE CELL (2018-2023)

CUSTOM-ART DISRUPTIVE KESTERITE-BASED (2020-2023)

Thank you for your attention!

15th Kesterite$^+$ & ReNewPV Workshop 2025

11. June – 13. June 2025

Berlin, Germany

Intrinsic point defects in kesterite-type CZTS and CZTSe: insights from theory

CZTS

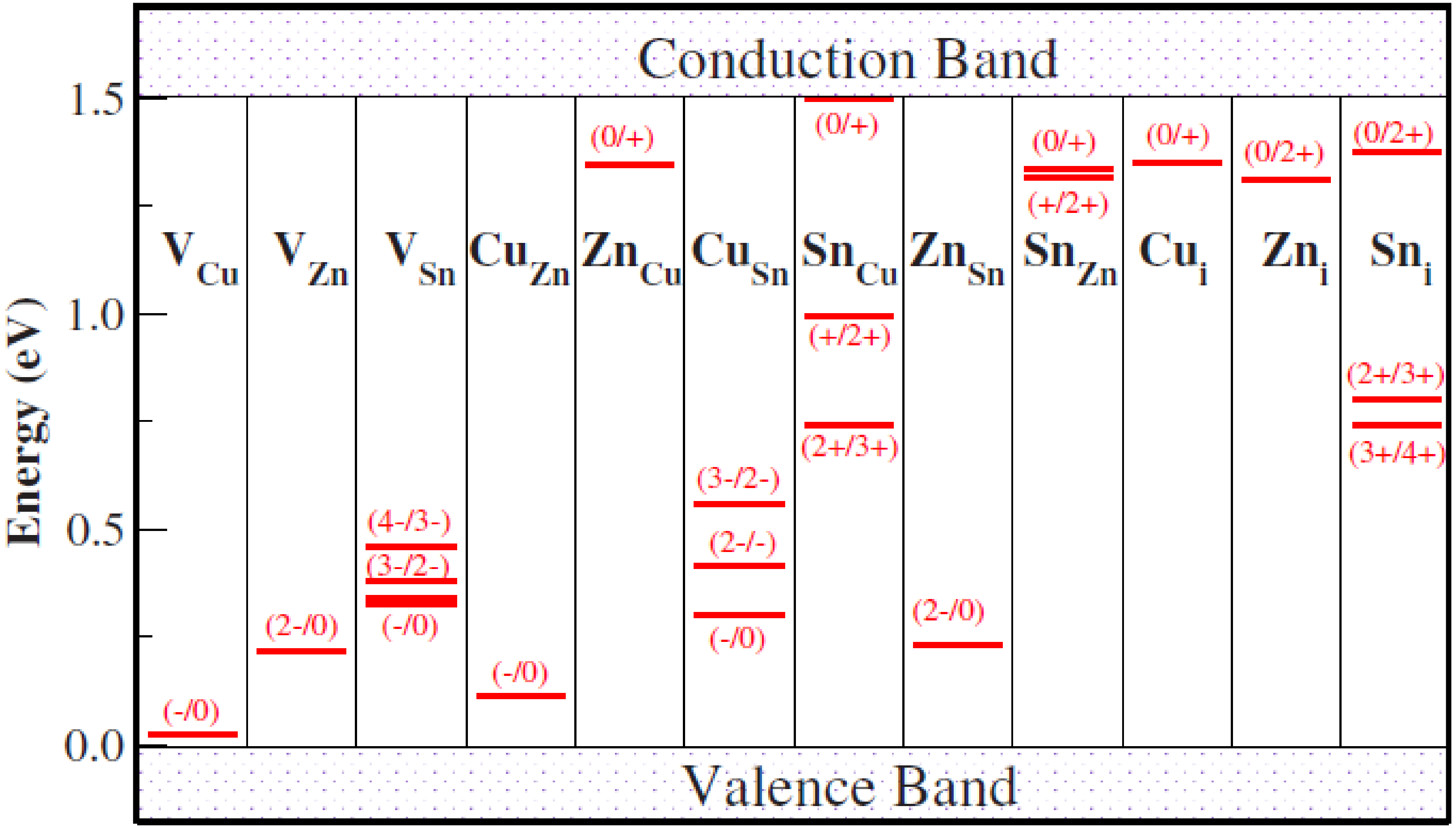

shallow defects → low SRH rates → beningn → „good“ defect
deep defects → high SRH rates → detrimental → „bad“ defect

intrinsic point defects

defects introduce energy levels (traps) in the band gap ➞ annihilate charge carriers (Shockley-Read-Hall recombination-SRH)

V_{Cu} ➞ shallow acceptor
Zn_{Cu} ➞ mid gap defect
Zn_{Sn} ➞ mid gap defect
Zn_i ➞ mid gap defect
Cu_{Sn} ➞ deep defect
Cu_i ➞ not favourable
Cu_{Zn} ➞(shallow) acceptor
Sn_{Zn} ➞ mid gap defect

intrinsic point defects in high concentrations (10^{19} – 10^{20} defects/cm^3)

➞ structural disorder

S. Chen et al, Phys Rev 81 (2010) 245204 *T. Maeda et al., Jpn. J. Appl. Phys. 50 (2011) 04DP07*

Effect of off-stoichiometry on band gap energy E_g

cation ratio plot

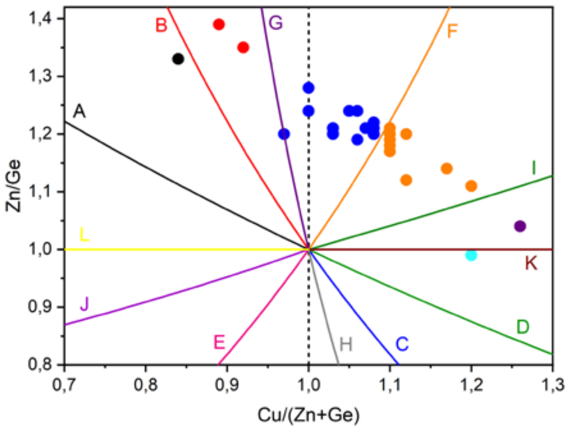

band gap energy E_g depends strongly on the off-stoichiometry (expressed by the catio ratios)

→ causes band gap fluctuations and electrostatic potential fluctuations in the absorber layer

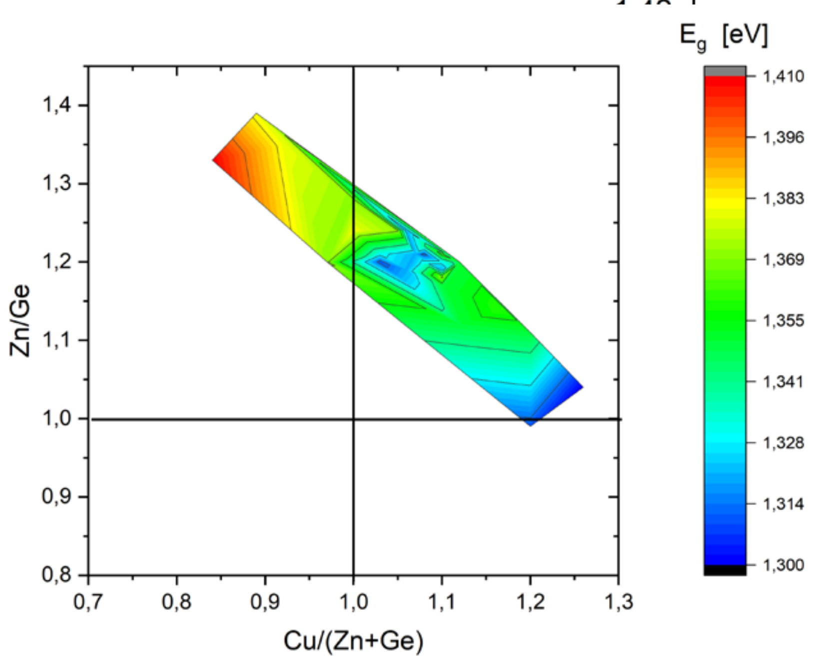

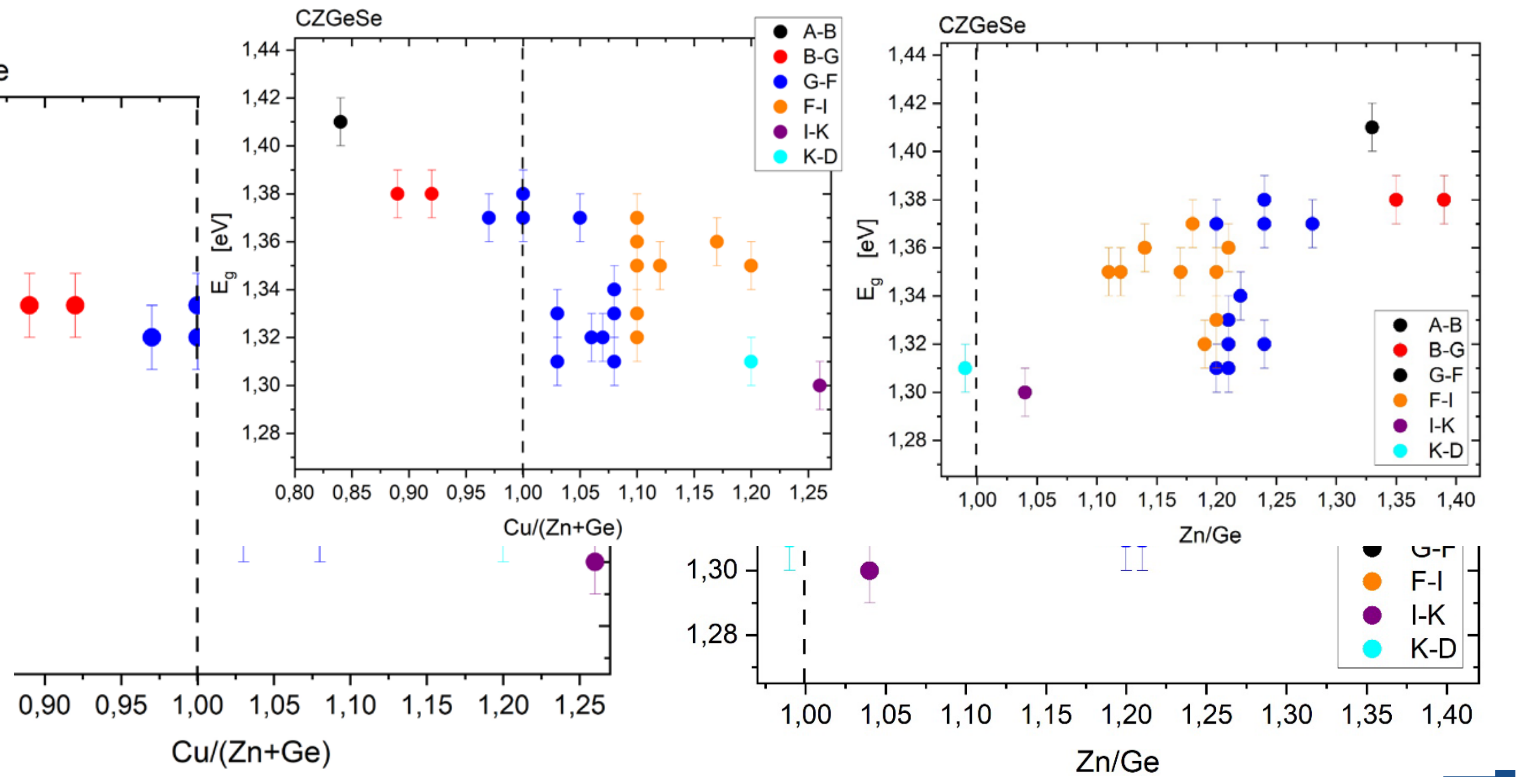

....

"One of the <u>**biggest advantages**</u> offered by **halide perovskites with respect to other semiconductor materials** is the **possibility to tune their absorption onset a la carte by ion replacement**…"

M. Anaya et al. Joule 1 (2017) 769-793

P. M. Woodward, *Acta Cryst. B 53* (1997) 32-43

perovskite family … perovskites

network of corner sharing octahedra

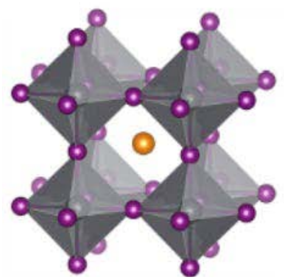

cubic perovskite
(space group $Pm\bar{3}m$)
e. g. $MAPbBr_3$

tetragonal perovskite
(space group $I\frac{4}{m}cm$)
e. g. $MAPbI_3$

orthorhombic perovskite
(space group $Pnma$)
e. g. $MAPbCl_3$

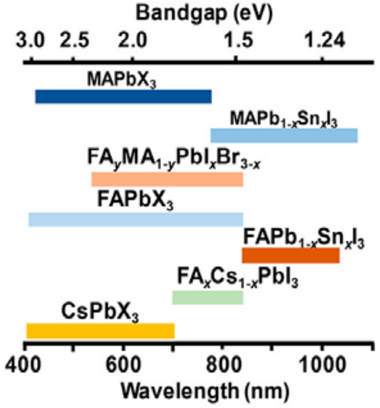

X=I, Br, Cl

One of the <u>**biggest advantages**</u> offered by **chalcogenide kesterites with respect to other semiconductor materials** is the **possibility to tune the absorption onset a la carte by ion replacement**
AND the long term stability of the material

B. Pamplin, Progr. Cryst. Growth Charact. 3 (1981)179-192

adamantine family … adamantines

network of corner sharing tetrahedra

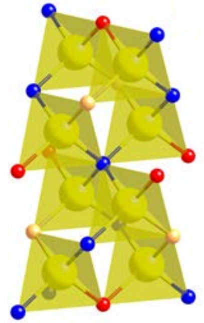

tetragonal stannite
(space group $I\bar{4}2m$)
e. g. Cu_2MnSnS_4

tetragonal kesterite
(space group $I\bar{4}$)
e. g. $Cu_2ZnGeSe_4$

orthorhombic wurtz-stannite
(space group $Pnm2_1$)
e. g. Cu_2MnGeS_4

monoclinic wurtz-kesterite
(space group Pn)
e. g. $Cu_2ZnSiSe_4$

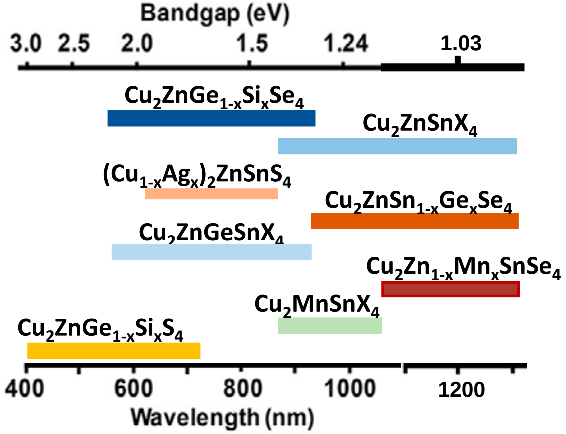

X=S, Se

Schorr, Sol. En. Mat. Sol. Cells 249 (2022) 112044

Flexible band gap energy tuning by ion replacement … in perovskites

ion replacement (cation/anion substitution) → formation of mixed crystals (solid solutions)

Are there similar challenges for perovskites?

replace I by Br in $MAPbI_3$ → $MAPb(I_{1-x}Br_x)_3$

T – x phase diagramm of $MAPb(I_{1-x}Br_x)_3$

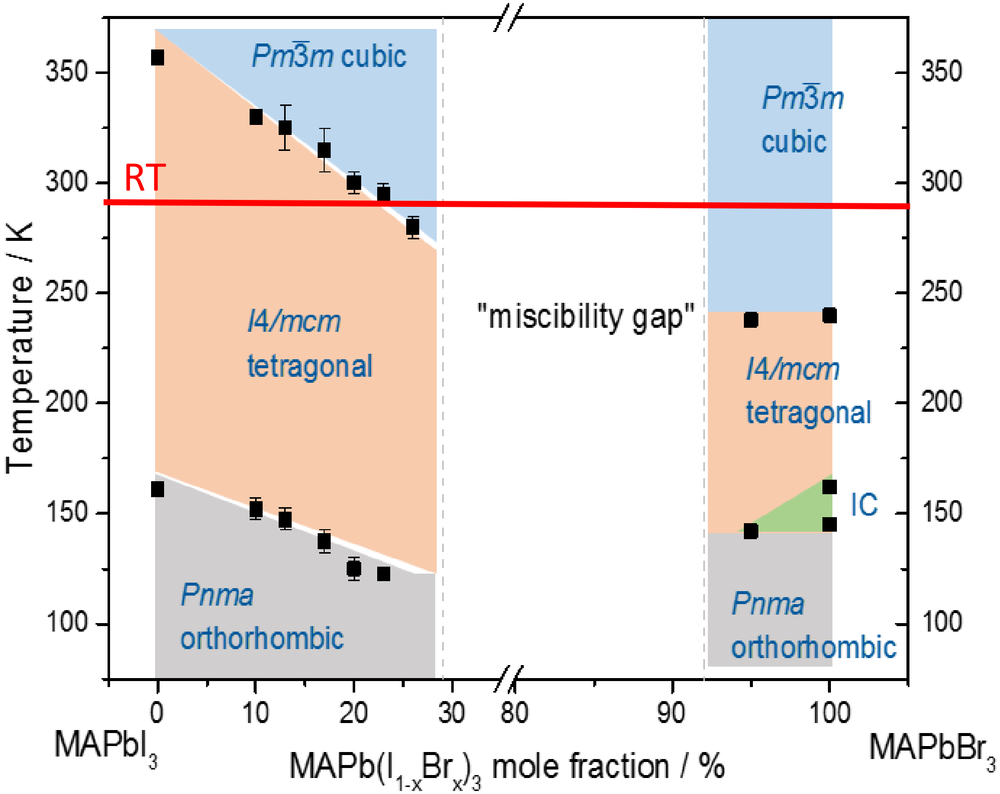

- crystal structure changes from tetragonal to cubic perovskite
- not a complete solid solution – miscibility gap

band gap energy E_g (determined by UV-Vis experiments)

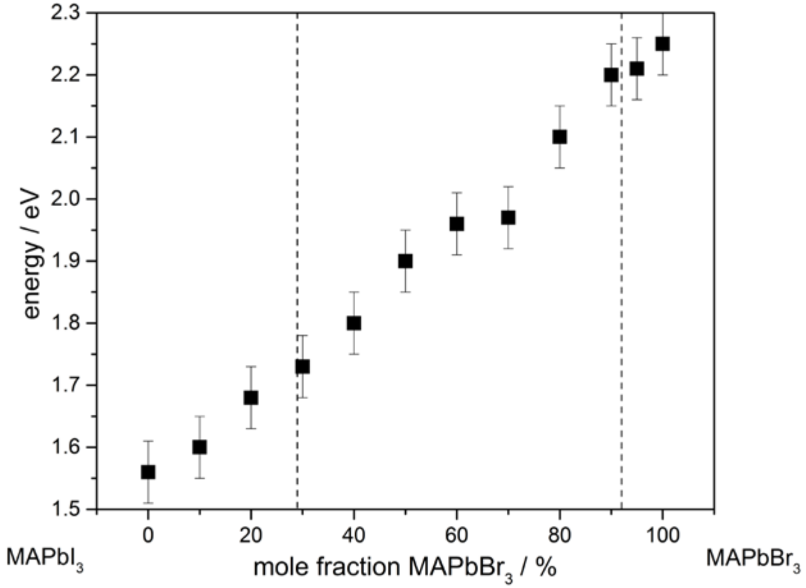

F. Lehmann et al., RSC Adv. 9 (2019) 11151